sustainability

Article

New Coal Char-Based Building Products: Manufacturing, Engineering Performance, and Techno-Economic Analysis for the USA Market

Suraj Prasad Pandey, Hua Yu, Chooikim Lau and Kam Ng *

Department of Civil and Architectural Engineering and Construction Management, University of Wyoming, Laramie, WY 82071, USA; spandey1@uwyo.edu (S.P.P.); hyu3@uwyo.edu (H.Y.); clau1@uwyo.edu (C.L.)
* Correspondence: kng1@uwyo.edu

Abstract: Common building products, i.e., thin brick and stone veneer, add the look of brick walls or the enduring charm of natural stones into buildings and houses without imposing a substantial increase in structural load. This study investigates the mechanical strength, durability, and economic feasibility of producing innovative char-based thin bricks and stone veneers. The char-based thin brick vacuum treated with hydrophobic liquid exhibits water absorption rates within the 4–7% range, displays durability against 50 freeze–thaw (F-T) cycles, and maintains a saturation coefficient below 0.6. In contrast, commercial thin bricks have water absorption of 9–12%. Treated char-based stone veneer has water absorption of 5.3% and an average compressive strength of 19.2 MPa, maintains its structural integrity throughout 50 F-T cycles, and exhibits a negligible linear shrinkage of approximately 0.01%. In contrast, commercial stone veneers have water absorption of 10–16%. These engineering properties meet the criteria as per ASTM standards C1088 and C1670 for thin brick and stone veneer, respectively. A techno-economic study was preliminarily conducted to examine the potential cost efficiency and cash flow in manufacturing these char-based building products. The manufacturing cost of USD 25.83 is lower than the average market price of 64.65 USD/sq. m. for thin bricks. The manufacturing cost of USD 32.65 is lower than the average market price of 129.17 USD/sq. m. for stone veneers. These comparisons present a compelling economic advantage for their commercialization. This comprehensive study has demonstrated the advantages of sustainable char-based stone veneers and thin bricks regarding engineering performance and economic benefits.

Keywords: char product; masonry veneer; engineering properties; net present value; internal rate of return; sensitivity analysis

check for updates

Citation: Pandey, S.P.; Yu, H.; Lau, C.; Ng, K. New Coal Char-Based Building Products: Manufacturing, Engineering Performance, and Techno-Economic Analysis for the USA Market. *Sustainability* **2024**, *16*, 1854. https://doi.org/10.3390/su16051854

Academic Editors: Amit Kenny and Mert Yücel Yardımcı

Received: 19 January 2024
Revised: 10 February 2024
Accepted: 20 February 2024
Published: 23 February 2024

Copyright: © 2024 by the authors. Licensee MDPI, Basel, Switzerland. This article is an open access article distributed under the terms and conditions of the Creative Commons Attribution (CC BY) license (https://creativecommons.org/licenses/by/4.0/).

1. Introduction

Thin bricks and stone veneers are common building products used primarily for decorating the external façade of a building or structure [1]. These products require less material for manufacturing and less labor for installation when compared to traditional bricks and natural stones. These inexpensive products bring the look of brick walls or natural stones to a building made from wood or other materials [2]. They have a maximum thickness of 44.5 mm for thin bricks [3] and 67 mm for stone veneers [4]. They are lightweight products and do not impose a substantial increase in dead loads for the buildings. In addition to aesthetic beauty, these products affect the temperature flow and humidity [5] between the atmosphere and the inside of the buildings. They act as an additional layer outside the main wall to provide insulation. This leads to a reduction in energy consumption [6] as the heat loss rate is slow compared to a building without an external cladding material. Consequently, there will be savings in cost and energy. Countries such as America, Canada, New Zealand, and England have experienced growing use of these products [6]. Some notable examples where such products are used include the University of Wyoming in America and the Electricity Museum in Portugal [6]. The lighter weight of these veneers compared to traditional bricks or natural stones leads to a reduction in storage and transportation expenses as well [7]. Wood sidings are another aesthetic material used for buildings [8], but properly designed and manufactured masonry veneers are durable to weather for a longer period [9] compared to wood sidings. Moreover, masonry veneers do not demand routine maintenance and rehabilitation such as painting of the surfaces, which is a common maintenance measure for wood sidings [8].

These thin bricks and stone veneers, often collectively referred to as veneers, act as a protection layer for concrete. In the absence of these, the exposed faces of concrete, due to their property of retaining moisture in their voids, facilitate the growth of algae and moss in the presence of damp conditions [10]. These release carbon dioxide during photosynthesis, and this carbon dioxide, along with humic acid produced because of putrefaction, leads to concrete corrosion, questioning the durability of the structures [11]. Using veneers with lower water absorption can be an essential measure to prevent deterioration. However, some veneers, if they do not have adequate water-resisting capacity, may still require the cleaning of algae and mosses attached to the surface using soapy water. This problem can be solved by introducing better technology and employing better raw materials with desirable outputs [12]. These veneers may also serve as a barrier in protecting the concrete from direct UV rays, thereby increasing the longevity of the structure [13].

These veneers are commonly concrete-based [14] and clay-based [15]. Concrete-based veneers are made with cement and natural aggregates [14]. The natural aggregates are sourced from mines by crushing the large rocks, which requires significant energy consumption (fuels) for operating heavy machinery equipment such as excavators and dumping trucks [16]. The crushed rocks then undergo grading processes to achieve suitable sizes for aggregates using vibratory feeders, conveyor belts, and screens [16]. This comprehensive procedure not only demands a considerable number of human resources, along with heavy machinery, but also raises concerns about the exploitation of natural resources [17]. Clay-based veneers are fired in a kiln at a very high temperature of 900 °C [18]. This makes them better in terms of fire-resisting capability [15]. However, this traditional production mechanism of using furnaces has been a growing issue in terms of environmental deterioration. Using furnaces at a large scale requires high energy consumption and generates greenhouse gases (e.g., CO_2) and/or hazardous gases (e.g., CO), which could cause environmental issues (e.g., ozone layer depletion) [19]. Additionally, mining of natural aggregates leads to the destruction of the habitat of native flora and fauna.

Therefore, there is an urgent need to find alternative raw materials/techniques that can reduce the consumption of natural aggregates. One such alternative is incorporating bottom ash and fly ash in the partial or complete replacement of natural aggregates. These materials are the byproduct of coal processing [20] and are procured at minimum cost, in contrast to the resource-intensive processes involved in the mining of aggregate sources and processing of natural aggregates. The literature studies have shown the promising potential of these materials in building and construction activities. Seav et al. [21] reported the possibility of incorporating coal-derived materials (i.e., bottom ash as a replacement for natural fine aggregates) in making concrete. Zhang et al. [22] found the suitability of using fly ash as a replacement for fine aggregate in making mortar satisfying the mechanical properties and durability conditions. These studies show the potential to minimize the exploitation of natural resources. However, the production process of bottom ash and fly ash involves the burning of coal and release of greenhouse gases into the atmosphere [20], and hence it may not be considered as a sustainable alternative to natural aggregates. Additionally, environmental advocates are raising their voices for a ban on the burning of coal. A recent study has shown a decline in coal mining activities [23] because industries are transitioning towards the use of renewable energy sources over coal. In response, the research community has developed an environmentally friendly process to make use of mined coal i.e., the pyrolysis process, which is a controlled chemical reaction [24]. The success of this technology is dependent on the wide-scale use of its resulting products, potentially enhancing the coal utilization efficiency. The resulting products of the pyrolysis process are pyrolysis oil, syngas, and char [25]. The pyrolysis oil and syngas are of high value [26] and are relatively expensive compared to char. Char, the left-over solid residue [27], is chemically stable in nature and if properly utilized offers a low-cost environmentally friendly alternative to the use of aggregates. Besides using coal-derived char, some other studies [28] have been carried out to examine a sustainable alternative (manufactured sand and coconut shell) to the use of natural aggregates. The feasibility of using such alternatives in making thin brick and stone veneer has received limited attention. It is worth noting that the present study is limited to determining the feasibility of incorporating char in making thin bricks and stone veneers.

Previous researchers [29–31] have successfully demonstrated the use of char for sustainable construction operations by replacing aggregates entirely and/or in part. Olayiwola and Ng [29] raised the possibility of incorporating coal-derived char as a partial replacement of sand in making bricks, along with the use of fly ash as an activator. Yu et al. [31,32] developed a method to completely replace the sand with coal-derived char in manufacturing bricks and also studied the effect of different curing temperatures on char-based bricks. Furthermore, other attempts have been presented by Yu et al. [30] to use coal-derived char for enhancing the engineering performance of conventional cement grout.

This study explores the potential use of char for addressing the environmental concerns raised by excessive use of natural aggregates and conventional manufacturing technology of using furnaces. Very few studies are available in the research community in regard to the manufacturing process of artificial masonry veneers. This study provides a simplified and in-depth manufacturing methodology along with comprehensive evaluation of engineering properties of the proposed char-based masonry veneers. The study also examines the effect of commercial adhesives compared to cement paste in increasing the shear bond strength of masonry veneers. Unlike previous studies, the present study is further extended to determine the economic feasibility of commercializing these char-based thin bricks and stone veneers. Three economic parameters—net present value (NPV), breakeven period or payback period (PB), and internal rate of return (IRR)—as the widely accepted practical tools, are adopted in this study to assess the economic feasibility and sensitivity analysis of these products [33]. This research unlocks new possibilities for using coal char in thin bricks and veneers, offering performance-matching commercial options. The flowchart summarizing the conducted study is shown in Figure 1.

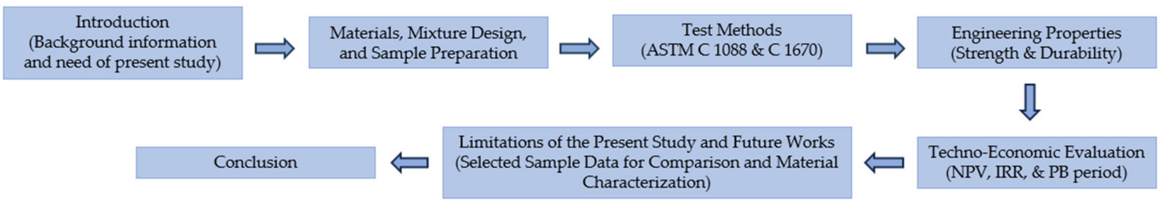

Figure 1. Flowchart showing different sections of the manuscript.

2. Materials, Mixture Design, and Sample Preparation

2.1. Materials

The materials used for making masonry veneers included pyrolysis char (PC), ordinary Portland cement (OPC) types I and II, superplasticizer (SP), and silica fumes (SF). PC is a coal-derived carbon-rich porous material obtained from coal pyrolysis and is incombustible. SP and SF were added as an admixture to improve workability, reduce water content, and increase the strength, and hence improve the durability, of the mix [34]. The SF used was greyish in color and amorphous micro-ionized grey silicon dioxide pozzolana procured from Diversified Minerals Inc. In contrast, the SP used was pale yellowish powder (Melflux 2651 F), which is a dried powder form of poly carboxylic ether and was procured from BASF construction additives.

2.2. Mixture Design for Char-Based Thin Brick and Stone Veneer

Thin bricks were designed by adopting the mix design developed by Yu et al. [32] for char-based building bricks, containing 40% char, 53.5% cement, 1.2% SP, and 5.3% SF at a water-to-binder ratio of 0.53. Based on this mixture design, investigation procedures were carried out on thin brick samples with thicknesses of 13 mm and 27 mm, chosen to mirror application scenarios in residential settings [35]. The char used in producing thin brick samples has 70% of its particles smaller than 300 μm and an average water content of 14%. ASTM standard C 1088 [3] was referred to when examining the engineering properties of manufactured char-based thin bricks.

Stone veneers were designed by adopting the mix design developed by Yu et al. [32] for char-based building bricks, containing 40% char, 53.5% cement, 1.2% SP, and 5.3% SF. Based on this mix design, investigation procedures were carried out on stone veneer samples manufactured at two variable water-to-cement (w/c) ratios of 0.53 and 0.70. The char used for producing stone veneer samples has 80% of its particles smaller than 300 μm and an average water content of 14%. ASTM standard C 1670 [4] was referred to when examining the engineering properties of manufactured char-based stone veneers.

Besides these standards, some other ASTM standards, as shown in Table 1, were also referred to when testing the engineering properties of thin bricks and stone veneers. In particular, the requirement of compressive strength for thin bricks is omitted in the ASTM standard C1088 due to their focus on aesthetics rather than load-bearing capacity, and accordingly, no compression test data are reported in this paper. Additionally, ASTM standard C1088 does not indicate the requirement of shear bond strength and linear drying shrinkage of thin bricks, and hence no test was carried out.

Table 1. Applicable engineering standards for examining the engineering properties of thin bricks and stone veneers.

Properties	Applicable Standards for Thin Bricks	Applicable Standards for Stone Veneer
Compressive strength	Not required	ASTM C1670, C31 [36], and C39 [37]
Water absorption	ASTM C1088 and C67 [38]	ASTM C67
Freeze–thaw	ASTM C1088 and C67	ASTM C1670, C31, and C666 [39]
Linear drying shrinkage	Not required	ASTM C1670 and C157 [40]
Shear bond strength	Not required	ASTM C1670 and C482 [41]

2.3. Sample Preparation for Thin Brick and Stone Veneer

The step-by-step manufacturing process for stone veneer and thin bricks is depicted in Figure 2. where essential raw materials for development were weighed first, followed by dry mixing for approximately three minutes in a laboratory mixer. After performing the dry mix, a predetermined quantity of water mixed with SP in a designated proportion was added to the rotating mixture for another three minutes to obtain a homogeneous mixture.

For manufacturing thin bricks, the wet mix was first placed in a rectangular steel mold up to a desired thickness. The mix was then compacted using a 3.3 kg cylindrical hammer having a length of 800 mm, with a square base having a 10 mm thickness and a cross-sectional area of 6800 mm^2. The compacted mass was then transferred to a hydraulic press machine to compress under 7 MPa pressure for one minute. This pressing action further enhances the particle compaction and densification process, as shown in Figure 2.

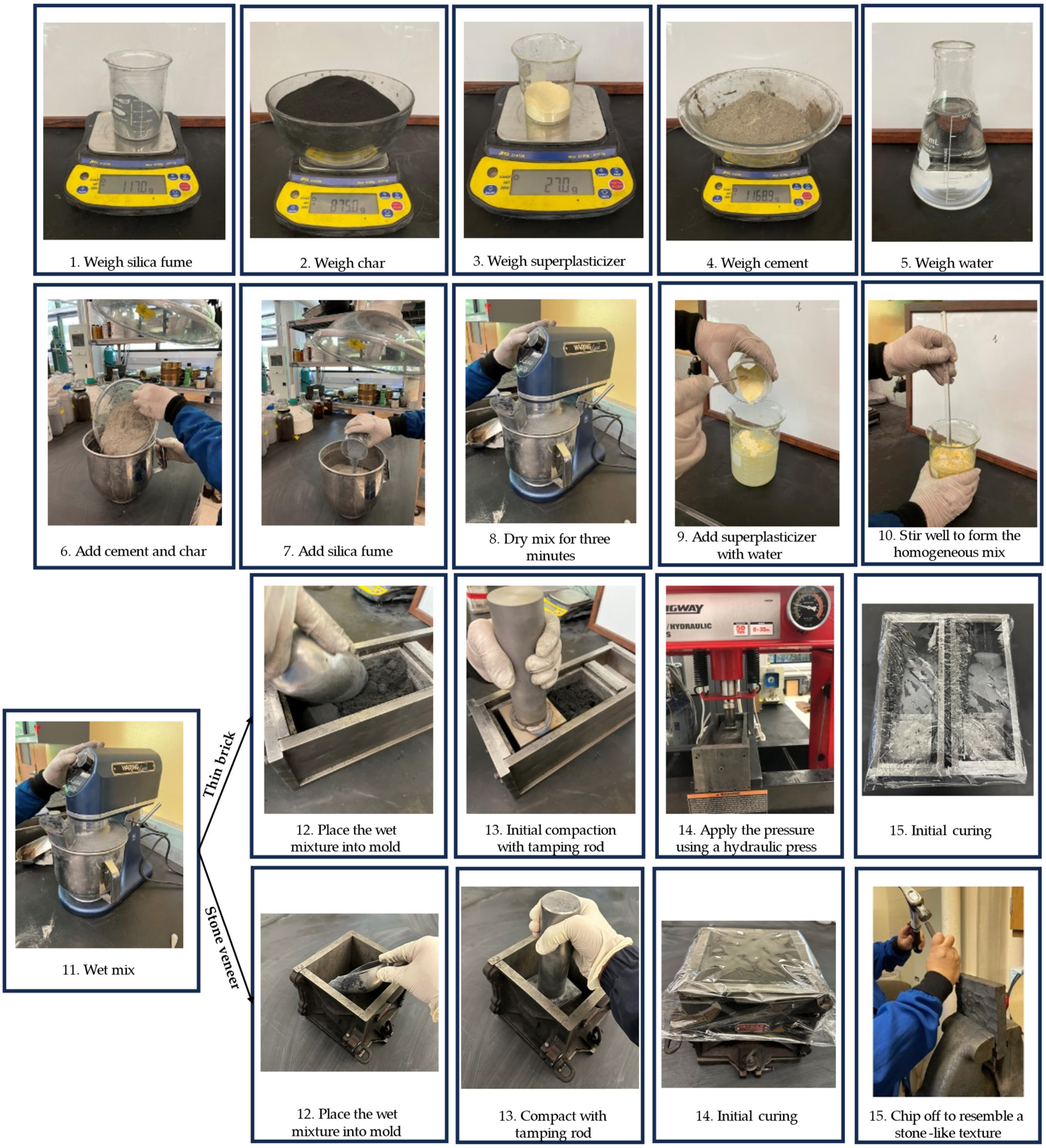

Figure 2. Detailed procedure for manufacturing thin bricks and stone veneers.

For manufacturing stone veneers, two different methods were introduced to develop a natural stone-like surface texture. The first method directly filled the mixture into plastic/rubber molds (Figure 3) with a stone-like texture on the bottom. The mixture was added in two layers, where each layer was compacted using a hammer like that used for manufacturing thin bricks to ensure the proper compaction and densification of the mixes in the molds.

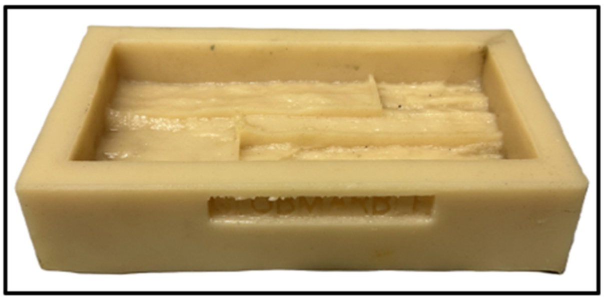

Figure 3. Commercial rubber mold for producing stone veneer.

The second method required two stages in manufacturing. The first stage involved the preparation of rectangular or square-shaped blocks by placing the mix on previously prepared steel molds, as shown in Figure 2, in two equal layers, where each layer was compacted using the same hammer as used for thin bricks. This compaction ensures the densification of the mixes in the molds. The second stage commenced after 28 days of curing in a humidifying chamber, and its details are outlined in a subsequent section. Following this stage, the mix was left to cure in the mold for one day.

After that, the stone veneer and thin brick were demolded from the respective steel mold. The demolded thin brick and the stone veneer were placed in the humidifying chamber for 28 days of curing. The humidity chamber provides the necessary moisture conditions with the added benefit of allowing control over the relative humidity. In the second stage of crafting stone veneers using the second method, the fully cured rectangular blocks underwent a process where a hammer was employed to chip away the surface (Figure 2) to create a natural stone-like texture.

The hydrophobic liquid (HL) treatment for the thin brick and stone veneer samples is proposed to make them resistant to water penetration and to increase their durability. For the treatment procedure, the prepared samples were submerged in hydrophobic liquid under a vacuum condition for 24 h, as similarly discussed by Yu et al. [32]. The samples undergoing the treatment process are referred to as treated samples, or otherwise as untreated samples, within the context of this study.

The manufactured char-based thin bricks (Figure 4a) had a dimension of L 193 × B 88.9 × T 13 mm. Similarly, the char-based stone veneers manufactured using the first method (Figure 4b) had a dimension of L 190 × B 100 × T 40 mm, and stone veneers manufactured using the second method (Figure 4c) had a dimension of L 152 × B 152 × T 40 mm.

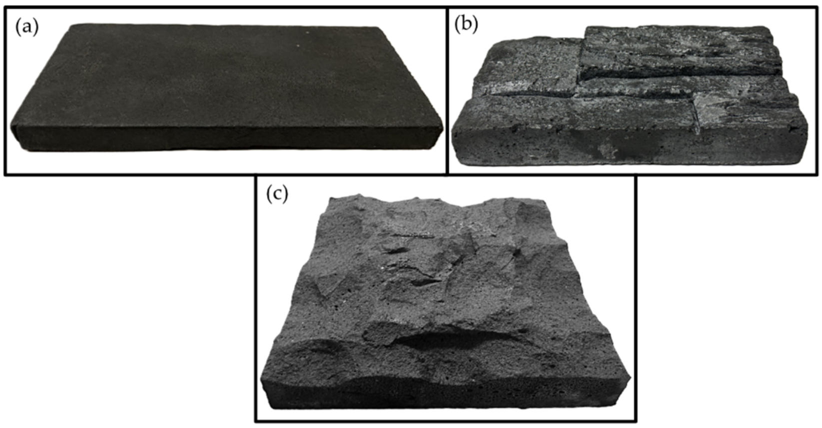

Figure 4. Pictures for char-based (**a**) thin brick, (**b**) stone veneer manufactured using the first method, and (**c**) stone veneer manufactured using the second method.

3. Test Methods

The ASTM standards C1088 [3] and C1670 [4] were followed to test the required engineering properties of char-based thin bricks and stone veneers. The cylindrical samples of diameter (D) 50 × height (H) 100 mm were prepared as shown in Figure 5a for testing the compressive strength of stone veneers. The samples for the compressive strength test were prepared following the ASTM standard C31 [36] and then laboratory testing was carried out following the ASTM standard C39 [37] using an automatic concrete compression testing machine as shown in Figure 5b. This compression machine is equipped with a touchscreen controller and is capable of controlling the rate of loading, break detection, and data collection. In our experiment, the loading rate of 0.49 kN/s was applied over the prepared cylindrical samples.

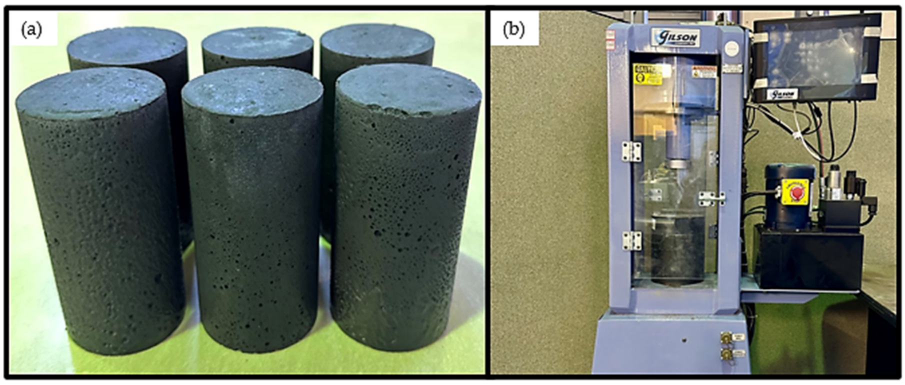

Figure 5. Compressive strength testing of stone veneer samples: (**a**) cylindrical samples, (**b**) compressive strength testing machine.

A water absorption test for thin brick and stone veneer was carried out following the ASTM standard C67 [38]. This test aims to determine the durability of produced samples in changing weather conditions [42]. The thin brick samples for the water absorption test have length (L) 95 × breadth (B) 90, with two different thicknesses (T) of 13 mm and 27 mm. The stone veneer samples prepared for the water absorption test had L 95 × B 90 × T 40 mm. Firstly, the samples were submerged in water at room temperature for 24 h as shown in Figure 6a, and subsequently, the samples were placed in boiling water as shown in Figure 6b for five hours. The ratio of the weight of the sample after five hours of submersion in boiling water to the initial dry weight of the sample multiplied by 100 gives the total water absorption.

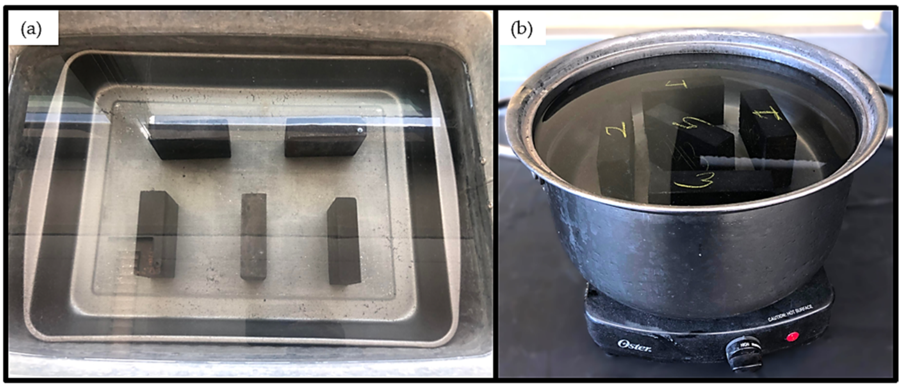

Figure 6. Water absorption test setup for thin bricks and stone veneers: (**a**) water absorption in cold water and (**b**) in boiling water.

The freeze–thaw test for thin bricks was conducted as per ASTM standard C67 [38]. The samples were first placed in a thawing condition for four hours as shown in Figure 7a before transferring them to a freezer in a freezing condition as shown in Figure 7b for the next 20 h. The freezer used in the experiments had a digital control panel and an air temperature of −10 °C was maintained inside the freezer. Five alternating cycles of freezing and thawing were executed in five days within one week, with the samples underwent air drying during the remaining two days. This procedure persisted for a total duration of 50 days. The presence of any cracks in samples was carefully checked in each cycle based on visual inspection.

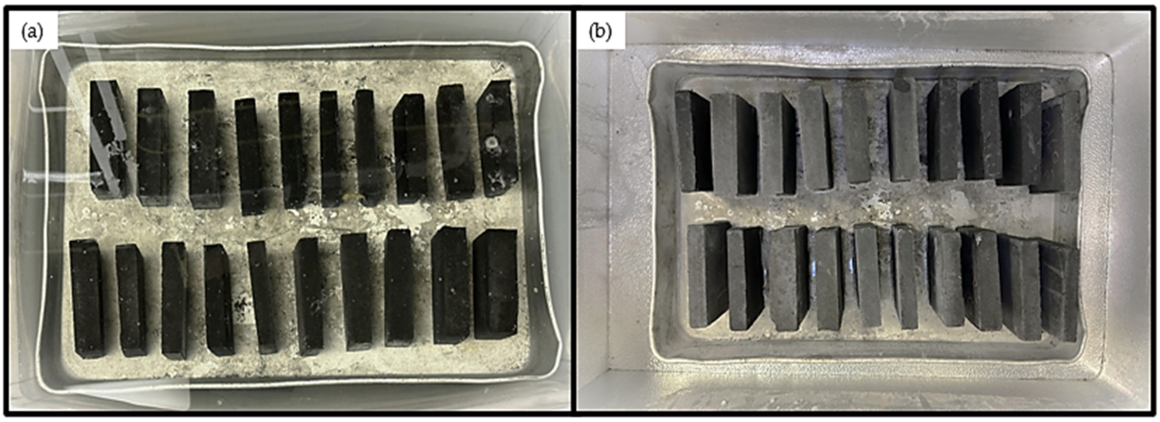

Figure 7. Freeze–thaw test setup for thin bricks: (**a**) thawing condition and (**b**) freezing condition.

For stone veneer, ASTM standard C666 [39] was followed for freeze–thaw tests. This method is an accelerated method for testing the freeze–thaw durability of stone veneer samples. The test samples had an average dimension of L 400 × B 78 × T 76 mm, as shown in Figure 8a. The freeze–thaw cycles were carried out in a freeze–thaw cabinet (Figure 8b), which simulates the cold and warm weather conditions. This freeze–thaw cabinet is fully automatic and is capable of performing up to eight freeze–thaw cycles in a day. In our experiment, the cabinet was set to alternate between −17.78 °C (freezing condition) and 4.44 °C (thawing condition) every five hours. During these five hours, an average of three hours were used for freezing and the remaining two hours were allocated for thawing. Then the samples were placed inside the cabinet in a rigid aluminum container (Figure 8c), where each sample was surrounded by 3 mm water. In a day, an average of five test cycles was carried out.

Figure 8. Freeze–thaw test setup for stone veneer samples: (**a**) cylindrical samples, (**b**) automatic rapid freeze–thaw testing machine, and (**c**) samples placed inside the freeze–thaw testing machine.

In addition, linear drying shrinkage of stone veneers was measured following the ASTM standard C157 [40]. Three samples having dimensions L 285 × B 55 × T 55 mm were prepared as shown in Figure 9a. The samples were stored in lime-saturated water, and the differences in length measurements using a length comparator (Figure 9b) were determined on the 7th day and 35th day from the date of casting. The length comparator was used to measure the length change of the specimen. This length comparator is equipped with a digital gauge and is battery operated to measure the length change. The ratio of the difference in length measurement to the length measurement taken at 7 days, when multiplied by 100, gives the shrinkage percentage of that sample.

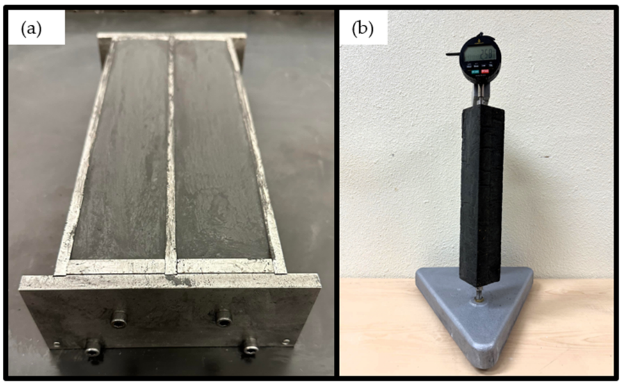

Figure 9. Linear drying shrinkage test setup for stone veneer samples: (**a**) samples prepared in the mold and (**b**) measurement of shrinkage readings using a comparator.

The shear bond test was performed on stone veneer samples to determine their ability to adhere against walls of building structures using cement paste and other adhesives as per ASTM standard C482 [41]. The prepared samples had a dimension of L 90 × B 90 × T 40 mm and were placed over the mortar block using cement paste having a w/c ratio of 0.36 as a bonding agent. Each test sample was held in an upright position with the aid of a fixture made of steel as shown in Figure 10a to prevent the tilting of the test sample during loading. This aforementioned fixture was fabricated within a laboratory setting as per the design consideration given in ASTM C482 [41]. An axial load was then applied on the stone veneer sample from the top, as shown in Figure 10b, to shear off the sample from the block, and this corresponding maximum shear stress was calculated as the shear bond strength of that sample.

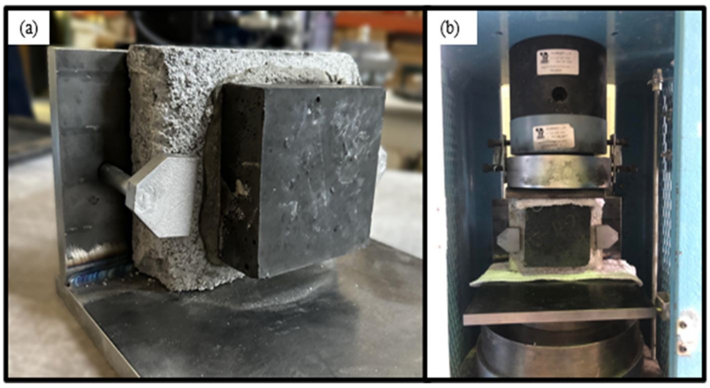

Figure 10. Shear bond test setup for stone veneer samples: (**a**) sample attached to mortar block and held in place with the suitable clamps (**b**) testing of shear bond strength.

4. Engineering Properties

The produced char-based thin bricks and stone veneers had density of 1463 kg/m^3 and 889 kg/m^3, respectively. The density of thin bricks and stone veneers was lower than that of commercial thin brick and stone veneers [43], positioning them as a favorable alternative to the commercial counterparts.

4.1. Compressive Strength

Thin bricks are non-load bearing and are attached to the building walls with the help of cement paste or some other adhesives. Their primary function is to enhance surface appearance rather than provide structural support. ASTM standard C1088 [3] also excludes the requirement for compressive strength.

In contrast, stone veneers may sometimes function as a partial load-bearing member in addition to providing an aesthetic appearance when used with a suitable support system. Accordingly, ASTM C1670 [4] specifies the minimum compressive strength of stone veneers as 15 MPa. The compressive strength of char-based samples at a water-to-cement (w/c) ratio of 0.7 (Csv, w/c = 0.7) was found to be 19.2 MPa and around 17% higher than 16.35 MPa at w/c = 0.53 (Csv, w/c = 0.53), as shown in Figure 11. The mix designs prepared at the w/c ratios of 0.53 and 0.70 satisfy the ASTM requirement of 15 MPa, as shown in Figure 11. This study indicates that within this range of w/c ratio, the stone veneer samples will comply with the specified compressive strength criterion, allowing manufacturers to have flexibility in the manufacturing process. The requirement of a higher w/c ratio for greater compressive strength may be attributed to the porous nature of char [44] as well as the higher surface area of char particles [45]. The porous nature of char contributes to high water-holding capability, thereby reducing the amount of free water available for the mix. Additionally, a high char surface area demands a higher amount of water for optimal bonding [46]. Proper water content supports effective particle dispersion, ensuring a more uniform distribution of cement throughout the mix and promoting enhanced bonding between particles [47]. Additionally, improved workability of the mix facilitates better placement and compaction, which contribute to increased strength [48]. In addition, the improvement in strength along with ductility and durability can be achieved with the use of fibers, as suggested by the study carried out by Zhang et al. [49], and broader applications can be investigated in the future.

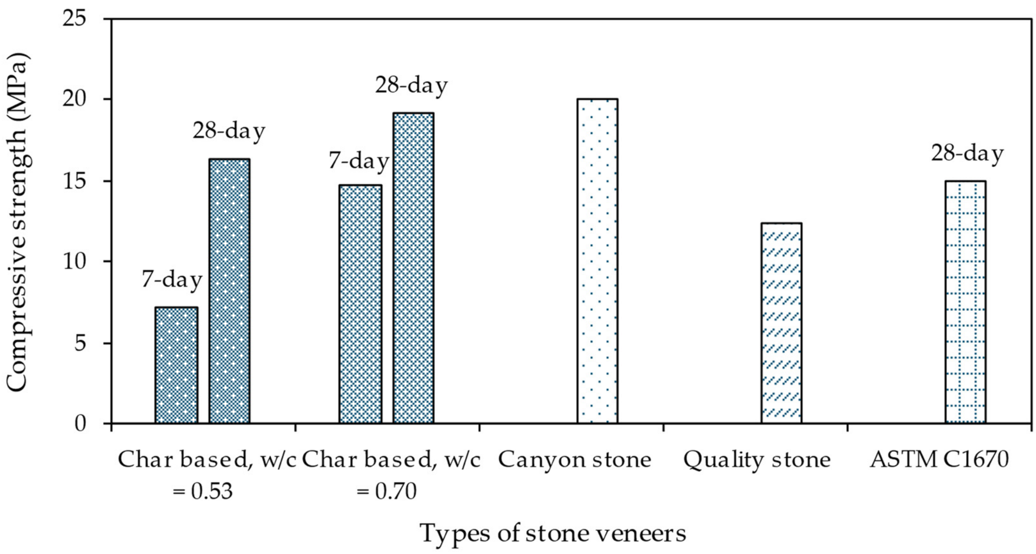

Figure 11. Comparison of compressive strength for different stone veneers.

The compressive strengths of commercial stone veneers, specifically those manufactured using Quality Stone Veneer (QS) [50] and Canyon Stone (CS) [51], are 12.4 MPa and 20 MPa, respectively. Notably, the compressive strength of char-based stone veneers at the 28 days surpasses the compressive strength QS of 12.4 MPa by 54.8%, and closely approaches that of CS of 20 MPa with only a 5% difference, highlighting the favorable performance of char-based stone veneers in terms of compressive strength. This indicates the suitability of the char-based stone veneers for their intended applications.

4.2. Water Absorption

The water absorption for untreated thin brick samples of various thicknesses and mix designs ranges from 20% to 27%. Conversely, for treated samples, the water absorption falls between 4% to 7%, as shown in Figure 12. The saturation coefficient for untreated half-thin brick samples spans from 0.60 to 0.85, whereas, for treated half-thin brick samples, the saturation coefficient lies between 0.30 and 0.60. The low water absorption and low saturation coefficient for treated half-thin brick samples indicate their superiority in terms of weather deterioration compared to untreated ones. The study was further extended to find the quantity of hydrophobic liquid required by each sample and to explain the behavior of hydrophobic liquid in making thin bricks water-resistant. For this, the weight of half-thin brick samples before and after hydrophobic liquid treatment was recorded. The results show that samples with a total surface area of 0.0255 m^2 require 50 g of hydrophobic liquid. Furthermore, the cross-section of the treated samples exhibits a notable resistance to water penetration. The study confirms that the hydrophobic liquid treatment enhances the water resistance of treated thin bricks.

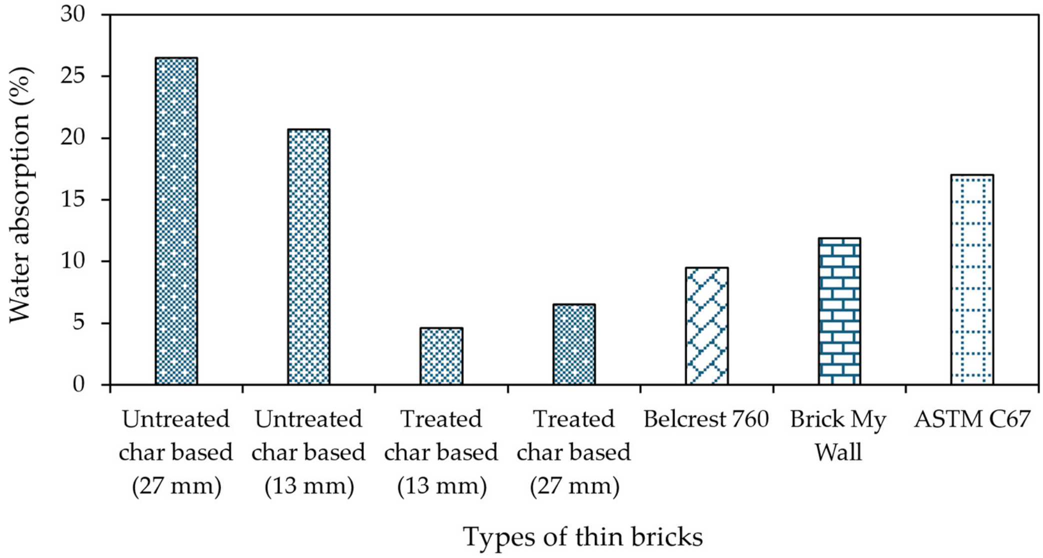

Figure 12. Comparison of water absorption for different types of thin bricks.

Compared to the two commercial thin bricks, the water absorption of treated char-based thin bricks is lower. Specifically, the thin brick manufactured by Belden the brick company, particularly the type Belcrest 760 [52] and Brick My Wall [15], have water absorption values of 9.50% and 11.90%, respectively. These findings highlight the suitability of treated char-based thin bricks compared to their counterparts in resisting deterioration due to weather.

For stone veneers, five half-block samples treated with hydrophobic liquid show an average water absorption of 5.13% with a saturation coefficient of 0.52. The water absorption values of commercial stone veneers, specifically QS [50] and CS [51], are 15.1% and 11.4%, respectively. The noticeably low water absorption values of char-based stone veneers compared to commercial ones, as shown in Figure 13, imply the better durability of stone veneer samples to seasonal variations throughout the year. This comparison indicates the potential benefits of char-based stone veneer for its intended application.

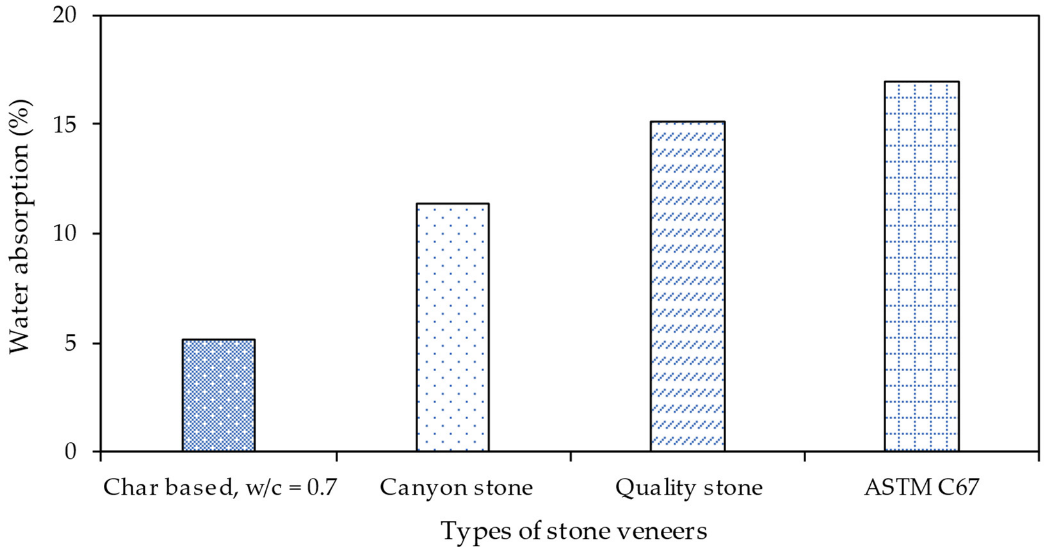

Figure 13. Comparison of water absorption for different types of stone veneers.

This resistance to water absorption also deters the growth of algae and molds on their surface. Algae and molds release enzymes and corrosive metabolites like acids. These acids react with concrete-binding materials and ultimately lead to the formation of low-strength materials [10]. The low-strength materials during the rainy season get washed away, leading to the weakening of the material. Additionally, thin bricks and stone veneers with low water absorption mean that they have the capacity to reduce moisture absorption and retention. In addition, this characteristic directly reduces the product's ability to conduct heat [53]. The present study lacks information regarding the treatment conditions of thin bricks and stone veneers. Alternatively, it is important to understand that commercial thin bricks and stone veneers can also be treated, potentially affecting their performance. This study focuses only on examining the viability of char-based thin bricks and stone veneers only. Comparisons are provided to complement the present study.

4.3. Freeze–Thaw Resistance

Both treated and untreated half-thin brick samples with a thickness of 13 mm successfully sustained the 50 freeze–thaw cycles, whereas for half-thin brick samples that were 27 mm thick, only treated ones passed the 50 freeze–thaw cycles. The untreated 27 mm thick samples sustained only 30 cycles. According to the layered distribution of pressure theory, the pressure on the top is highest and decreases as it descends beneath the surface [54]. This phenomenon results in more uniform and efficient pressing under a pressure of 7 MPa during the manufacturing process for thin bricks having a thickness of 13 mm in comparison to those having a thickness of 27 mm. This pressing reduces the void spaces within the compacted mixture, ultimately yielding a denser structure. Thin bricks that are denser have fewer interconnected pore spaces, leading to a decrease in the accumulation of pore water. The reduction in the accumulation of pore water assists in preventing damage caused by expansion in freezing conditions [55].

To revalidate these findings, freeze–thaw tests were carried out on untreated half-thin brick samples with varying thicknesses, including 55 mm, 27 mm, 22 mm, 19 mm, and 13 mm. The results indicated that 27 mm and 54 mm are more susceptible to failure than 13 mm, 19 mm, and 22 mm samples, further emphasizing the significance of density of thin bricks in influencing the durability performance. The study recommends greater pressing pressure during manufacturing of 27 mm thin bricks to increase their freeze–thaw resistance and suggests further study to evaluate these findings.

For stone veneers, the freeze–thaw test was carried out on treated samples. The reason behind this is that stone veneer samples have a thickness greater than 27 mm, and these are produced from a wet mixture. These treated stone veneer samples successfully sustained the 50 freeze–thaw cycles. The commercial thin bricks manufactured by Belden, the brick company, particularly Belcrest 760 [52] and Brick My Wall [15], and stone veneers manufactured by QS [50] and CS [51], also exhibited the durability of manufactured samples up to 50 freeze–thaw cycles. This study indicates the comparable quality of the char-based products in terms of freeze–thaw durability.

Based on the water absorption and freeze–thaw test results, the treated samples of thin bricks and stone veneers have satisfactory engineering properties compared to relevant ASTM standards and commercial ones. Since ASTM C1088 [3] exempts the requirement of a water absorption assessment for thin bricks, provided five samples pass the freeze–thaw test, and by the findings obtained from the freeze–thaw test, untreated samples with thicknesses ranging from 13 mm to 22 mm were also deemed suitable for their application in specified environmental conditions.

4.4. Linear Drying Shrinkage

The test results for treated stone veneer samples show an average linear change of 0.01%. The average linear shrinkage for char-based stone veneers is within the permissible range of 0.1%, as specified in ASTM standard C157 [40]. This result means that the produced product will show negligible variation in dimensions due to seasonal variations, maintaining the products integrity over time. The fact that the product has very low linear shrinkage indicates its potential application in intended places and that it is unlikely to experience deterioration. The study lacks recorded data for commercial stone veneers, precluding any comparative analysis.

4.5. Shear Bond

The shear bond test was performed on treated stone veneer samples. The 7-day shear bond strength of the treated sample was 0.75 MPa, which is above the ASTM requirement of 0.35 MPa, suggesting the reliability of these products for their intended applications. This shear bond strength exhibited by char-based stone veneers is higher than the shear bond strengths of QS (0.34 MPa [50]) and CS (0.4 MPa [51]). Rizaee et al. [43] performed a shear bond strength test on stone veneers, specifically Eldorado Brick (EB) and Dutch Quality (DQ), and found the average shear bond strengths were 0.15 MPa and 0.23 MPa, respectively. These recorded values are lower than those observed in treated char-based stone veneers, as shown in Figure 14.

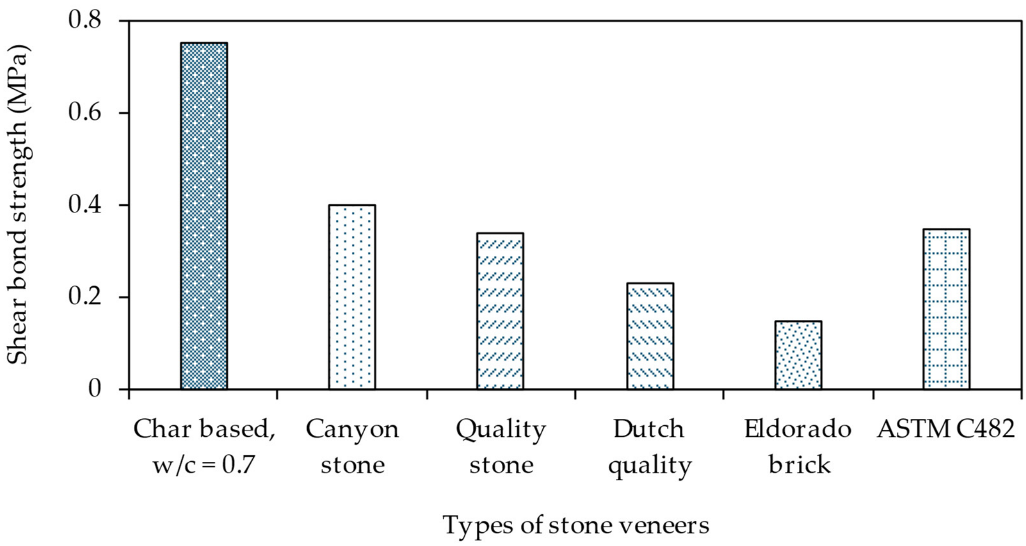

Figure 14. Comparison of shear bond test for different types of stone veneers using conventional cement mortar/paste.

To further improve the shear bond strength of treated stone veneer samples, commercial bonding materials, specifically Latpoxy stone adhesive and Baucer polymer cement, were employed. The shear bond strength of treated char-based samples using Latpoxy stone adhesive (CbL) is 2.82 MPa, and using Baucer polymer cement (CbB), the shear bond strength is 2.73 MPa. Rizaee et al. [43] also used the polymer-based adhesive to improve the shear bond strength of EB and DQ. The recorded shear bond strengths for EB (EBP) and DQ (DQP) are 2.22 MPa and 2.11 MPa, respectively. These shear bond strength values are still lower than those shown by char-based stone veneers when polymer as an adhesive was used in place of cement paste, as shown in Figure 15.

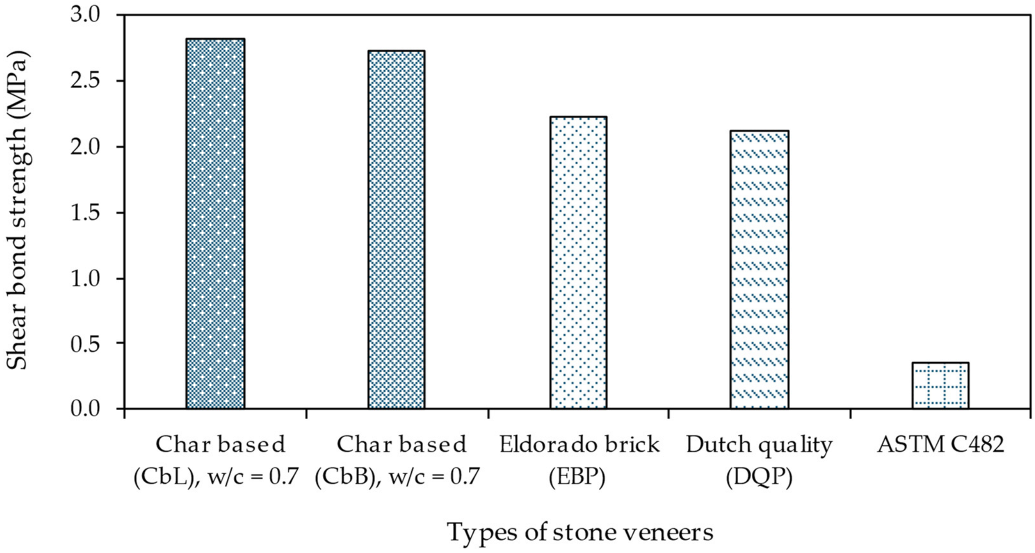

Figure 15. Comparison of shear bond strength of various types of stone veneers using polymer-based adhesives.

5. Techno-Economic Evaluation

Techno-economic analysis is a systematic approach used to evaluate the profitability and practicality of the implementation of any project. It considers capital expenditure, cash outflows, and cash inflows. Cash outflows can be quantified in terms of fixed cost and variable cost. In contrast, cash inflows usually are the revenue a company makes after selling their product. The most general approach used for measuring economic viability includes net present value (NPV), break-even period, and internal rate of return (IRR) [56].

NPV calculates all the future cash flows as the present value and subtracts capital expenditure from this value, as given by Equation (1). If NPV is greater than or equal to zero, then the project is considered feasible; else it is considered not feasible [56], as per Equation (1).

$$\mathrm{NPV} = \frac{\sum \text{Cash flow of each year}}{(1+\mathrm{i})^{\mathrm{n}}} - \mathrm{C_o} \quad (1)$$

where C_o represents the capital expenditure or initial investment, i represents the discount rate, and n represents the time period over which the project is aimed to continue.

The breakeven period [56] is the total number of years required for the cumulative expenditure of the company to equal cumulative revenues, and any revenue generated beyond that point is the profit earned by a company. To find the breakeven period, the cumulative cash flows are plotted on the *y*-axis and time in years is plotted on the *x*-axis. The point where the resulting line diagram intersects the *x*-axis is determined as the breakeven period for that project.

IRR [56] means the expected rate of return that a company can expect after investing in a particular project. It is calculated by making NPV equal to zero and back calculating the i given by Equation (1). The back calculated value i is the required IRR (r).

The economic analysis was carried out considering a project life of 15 years. The period of 15 years was used considering the significant investment in land and infrastructure and the service life of the specialized equipment [57].

Additionally, a series of sensitivity studies was conducted to determine the economic incentives of this project concerning the total capital expenditure, product price, cement cost, hydraulic lime (HL) cost, production rate, and fixed cost. Sensitivity studies were carried out on sensitive parameters of the project. Sensitive parameters were identified based on detailed cash flow analysis, and then analysis was performed by fluctuating the range of sensitive variables [58] such as capital expenditure, product price, production rate, OPC price, HL price, and fixed costs. This process allowed us to better account for the uncertainties associated with the project.

5.1. Techno-Economic (TE) Analysis of Thin Brick

The US market size of thin brick is assumed to be 50% of the market size of bricks i.e., USD 184 million [59], and the scenario in this study is expected to capture approximately 2.5% of the market size i.e., a revenue of USD 5.76 million. Techno-economic analysis of thin brick is conducted based on the preliminary manufacturing process. For a unit producing 4,800,000 pieces of thin bricks (L 193 × B 89 × T 13 mm) per year, which is equivalent to 1556.7 metric tons (1716 US tons) of thin bricks from PC, OPC type-I, SF, SP, and HL, the total capital expenditure is estimated at USD 7,330,316. This total capital expenditure encompasses the direct cost and indirect cost. Table 2 summarizes the production cost estimates for 1716 tons of thin brick annually. The direct cost of USD 4,536,279.16 is calculated based on the equipment and components required for the manufacturing along with the purchase of land and construction of a factory. The estimated cost of acquiring 5 acres (20,234 sq. m.) of land in Gillette, Wyoming, is USD 130,000 [60]. The construction expenses are computed at a rate of 8.94 USD/sq. m. (96.23 USD/sq. ft.) [61], amounting to USD 2,886,990 for a project covering 2787 sq. m. (30,000 sq. ft.). An additional 25% of total capital expenditure is allocated for contractor fees, and 7% of total capital expenditure is earmarked for architectural fees, resulting in a total expenditure of USD 3,861,349.34. The indirect cost of USD 490,436.84 is estimated for the first plant, with many uncertainties in manufacturing the thin brick (estimated at 90% of the equipment and component purchase cost). The indirect cost includes engineering services, equipment rentals, procurement, freight, taxes, and contingencies. It should be noted that the indirect cost can be reduced when the project maturity increases.

Table 2. Summary of cost estimates for producing 1556.7 metric tons (1716 US tons) of thin bricks per year.

Item	Description	Amount
A	Total capital expenditure (i.e., total Cap Ex)	USD 7,330,716.00
	Direct expenditure of total Cap Ex	USD 4,536,279.16
	Indirect expenditure of total Cap Ex	USD 490,436.84
	Working capital at 20% of total revenue (only in year 0)	USD 1,152,000.00
	Startup cost at 20% of total revenue (only in year 1)	USD 1,152,000.00
B	Raw materials (char, cement, silica fume, and SP)	389,096.53 USD/year
	Utility (water and electricity)	15,379.47 USD/year
	Subtotal	404,476.00 USD/year
D	Labor (total 1920 h per year) + Administrative cost	1,120,788.48 USD/year
	Maintenance (4% of Cap Ex)	293,228.64 USD/year
	Lab support cost (5% of Labor)	56,039.42 USD/year
	Plant overhead (10% of labor, maintenance, and lab)	147,005.65 USD/year
	Taxes and insurance (1% of Cap Ex)	73,307.16 USD/year
	Subtotal	1,690,369.36 USD/year
E	Total manufacturing cost (fixed cost + variable cost)	2,094,845.36 USD/year
F	Total manufacturing cost (fixed cost + variable cost)	0.44 USD/pc
G	Product price	1.20 USD/pc
H	Total revenue	5,760,000.00 USD/year

For an average product price of 1.20 USD/pc or 64.65 USD/sq. m. (6.0 USD/sq. ft.) of char-based thin bricks, which is comparable to the average prices of equivalent commercially available thin bricks, as shown in Table 3, the total revenue is estimated at 5,760,000 USD/year. Taking 20% of the total revenue, the working capital and startup capital are estimated each at USD 1,152,000.

Table 3. Price per square foot of commercial thin bricks.

Manufacturing Company	Price per sq. m.	Price per sq. ft.
Daltile	USD 71.04	USD 6.60 [62]
Brick my wall	USD 45.10	USD 4.19 [15]
Menards versatile royal thin bricks	USD 77.82	USD 7.23 [63]
Average price	USD 64.65	USD 6.0

Our research outcomes indicate that 1741 metric tons (1919.20 US tons) of raw materials (including water) are required to yield 1556.7 metric tons (1716 US tons) of thin bricks. For the thin brick consisting of 1PC:1.34OPC:0.13SF:0.03SP:0.04HL, 525.26 metric tons (579 US tons) of PC, 702.16 metric tons (774 US tons) of OPC, 70.76 metric tons (78 US tons) of SF, 15.78 metric tons (17.40 US tons) of SP, and 393.54 metric tons (433.80 US tons) of HL are required per year. The total price of procuring these materials is as shown in Table 4.

Table 4. Table showing calculation of total price of raw materials [64–68] used in the production of thin bricks.

Item	Unit Price per metric ton (US ton)	Required Quantity in Metric ton (US ton)	Total Price
Pyrolysis char	USD 44.092 (USD 40)	525.26 (579)	USD 23,160
Ordinary Portland cement	USD 132.304 (USD 120)	702.16 (774)	USD 92,880
Silica fume	USD 1554.355 (USD 140)	70.76 (78)	USD 10,920
Superplasticizer	USD 992.282(USD 900)	15.78 (17.4)	USD 15,660
Hydrophobic liquid	USD 626.44 (USD 568.18)	393.54 (433.8)	USD 246,476.53

The unit water cost is determined at 1.22 USD/thousand liters (Tliters) (4.63 USD/thousand gallons (Tgallons)) in addition to a fixed monthly cost of USD 127.04 [69]. The total water required in one year (11 working months) to produce 1716 tons of thin brick is calculated as 55.6 Tliters (14.70 Tgallons), including an additional 50% for some other applications, and the total annual water cost is estimated at USD 1465.50. Electricity is needed to power the ball mills, conveyor system, pan mixer, brick-making machine, automatic pallet jack, water pump, and dust collection equipment. The unit electricity cost is determined at 0.09311 USD/kWh in addition to a fixed monthly cost of USD 40.73 [69]. The total electricity per year consumption to produce 1556.7 metric tons (1716 US tons) of thin brick (11 working months) is determined as 143,184 kWh, and the total electricity cost is estimated at 13,913.97 USD/year. Adding all variable costs yields a total variable cost of 404,476 USD/year (Table 5).

Table 5. Rate of employees as per the US Bureau of Labor Statistics for Wyoming [70].

Description of Work	No.	Rate	Amount	Remarks
Construction managers	1	USD 45.31	USD 45.31	Rate per hour
First-line supervisors of production and operating workers	1	USD 42.97	USD 42.97	Rate per hour
mixing and blending machine setters, operators, and tenders	5	USD 22.16	USD 110.80	Rate per hour
Helpers-production workers	5	USD 20.18	USD 100.90	Rate per hour
Sales workers	1	USD 14.64	USD 14.64	Rate per hour
Accountants and auditors	1	USD 35.58	USD 35.58	Rate per hour
Drivers	1	USD 14.64	USD 14.64	Rate per hour
Subtotal			USD 364.84	Rate per hour

Eight hours of labor shifts are suggested to produce thin bricks, and the production is continued for five days a week. Hence, the total number of working hours per year (11 working months) for 8 h/day shifts is 1920. For one construction manager, one supervisor, five machine operators, five helpers, one sales worker, one accountant, and one driver per shift at a variable wage rate, as shown in Table 5 [70], the combined hourly pay is USD 364.84. Hence, the yearly pay considering 1920 working hours in a year is USD 700,492.80. If 60% of the wage is considered for overtime, benefits, and supervision, the total labor wage and other benefits is USD 1,120,788.48, as presented in Table 2.

The annual maintenance cost of USD 293,228.64 is determined as 4% of capital expenditure. The yearly cost of laboratory support is estimated at 5% of total labor cost or USD 56,039.42. The plant overhead cost is the total cost involved in operating all thin brick production facilities, and the annual plant overhead cost of USD 147,005.65 is estimated to be 10% of the total labor cost, maintenance cost, and laboratory cost. Taxes and insurance costs of USD 73,307.16 are estimated at 1% of the total capital expenditure. Adding all fixed costs yields a total annual fixed cost of USD 1,690,369.36 (Table 2). Combining the total fixed cost and variable cost, the total manufacturing cost is 2,094,845 USD/year. This is equivalent to 1202.65 USD/ton, which breakdowns as 0.44 USD/pc or 25.83 USD/sq. m. (2.40 USD/sq. ft.).

The analysis shows that the percent breakdown of the annual manufacturing cost of USD 2,094,845 consists of a total fixed cost of USD 1,690,369.36 (80.7%) and a total variable cost of USD 404,476 (19.3%). The variable cost consists of PC cost (1.11%), OPC cost (4.43%), SF cost (0.52%), SP cost (0.75), HL cost (11.77%), water (negligible), and electricity (0.01%). The combined OPC and HL cost, exceeding 15% of the total manufacturing cost, plays a significant role in the TE analysis, determining the feasibility of this project. Likewise, the analysis shows that the combined OPC and HL cost is 66% of the total variable cost, further signifying the importance of the combined OPC and HL cost in this project.

A cash flow analysis was conducted using the capital expenditure and cost estimates summarized in Table 2. Before manufacturing thin brick in year 1, the total capital expenditure of USD 7,330,716 is considered in the following distributions: 25% in Year −2, 50% in Year −1, and 25% in Year 0. The working capital of USD 1,152,000 is spent in Year 0 and will be returned at the end of the project in Year 15, with the expectation that the project will become profitable over the 15-year period, allowing for the return of the working capital at the project's completion. Hence, Figure 16 shows the negative cash flow values from Years −2 to 0 and a relatively higher positive cash flow in Year 15. The modified accelerated cost recovery system (MACRS) is utilized to allow the recovery of the capital expenditure as an asset with the following percent distributions over six years: 20%, 32%, 19.2%, 11.52%, 11.52%, and 5.76% for Years 1 to 6, respectively. The depreciation amount for each of these six years is calculated based on the respective percent distribution concerning the total capital expenditure. Considering a new corporate tax of 21%, the depreciation credit is calculated by multiplying 21% by the depreciation amount.

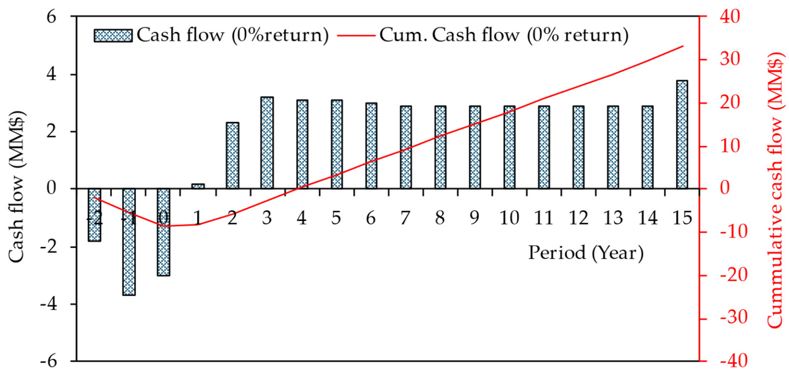

Figure 16. The cash flow analysis results for thin bricks considering a 0% return.

The annual revenue is estimated at USD 5,760,000 (see Table 2). However, it is assumed that the new plant will only reach 50% and 75% of its total capacity in Years 1 and 2, respectively, and the annual revenues are reduced to USD 2,880,000 and USD 4,320,000, respectively. The start-up cost of USD 1,152,000 is considered an expense in Year 1. The total manufacturing cost of USD 2,094,845 is included in Years 3 to 15, while only 50% and 75% of the manufacturing cost are accounted for in Years 1 and 2. Next, the annual margin, defined as the difference between total revenue and total expenses, is calculated for each year.

The tax liability per year is calculated by multiplying the annual margin by the 21% corporate tax. For a 0% return rate, the yearly cash flow is calculated by summing each year's total capital expenditure, working capital, depreciation credit, margin, and tax liability. The cash flow is accumulated from Years −2 to 15 and plotted along with the annual cash flows in Figure 16. The cumulative cash flow begins at a negative value of −USD 1,830,000 in Year −2 and reaches the maximum negative value of −USD 8,480,000 in Year 0, before breakeven in Year 4. Similarly, to calculate discounted cash flows, a discount rate of 7% is chosen, which is higher than the prevailing discount rate of 5.5% [71], as a precautionary measure to account for potential uncertainties. For the percent return or discount rate of 7%, the annual cash flow is reduced to the present value, as shown in Figure 17. Likewise, the yearly present value is accumulated, and the cumulative current value is plotted in Figure 17. The cumulative present value begins at −USD 2,100,000 in Year −2, reaches the maximum negative value of −USD 9,000,000 in Year 0, and breakeven is in Year 5.

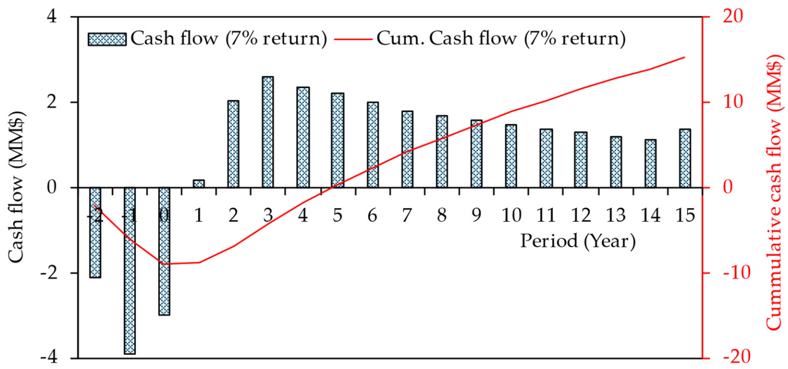

Figure 17. The cash flow analysis results for thin bricks considering a 7% return.

5.2. Sensitivity Analysis for Thin Brick

Table 6 shows the eleven cases and the base case described in previous paragraphs. The sensitivities are evaluated in terms of net present values (i.e., cumulative present value) in Year 15 for 0% and 7% return rates (NPV0 and NPV7, respectively).

Table 6. Sensitivity studies for thin bricks on the net present value and the internal rate of return across varied capital expenditure, production rate, product price, and raw material costs.

Case	Capital Expenditure (MM$ *)	Product Rate (Nos./hour)	Product Price (USD/pc)	Ordinary Portland Cement Cost (USD/ton)	Hydrophobic Liquid Cost (USD/ton)	NPV0 (MM$)	NPV7 (MM$)	IRR (%)
Base	7.33	2500	1.20	120.00	568.18	33.27	15.21	22.15
1	5.50	2500	1.20	120.00	568.18	34.71	16.85	26.51
2	9.16	2500	1.20	120.00	568.18	31.82	13.56	18.96
3	7.33	2500	0.60	120.00	568.18	3.52	−1.47	4.39
4	7.33	2500	0.72	120.00	568.18	9.47	1.86	9.79
5	7.33	2500	1.80	120.00	568.18	63.01	31.89	30.36
6	7.33	2500	1.20	144.00	568.18	33.06	15.08	22.05
7	7.33	2500	1.20	144.00	681.82	32.5	14.76	21.79
8	7.33	1250	1.20	120.00	568.18	3.52	−1.47	4.39
9	7.33	2125	1.20	120.00	568.18	24.34	10.2	18.51
10	7.33	2500	1.20	120.00	568.18	38.27	18.25	24.68
11	7.33	2500	1.20	120.00	568.18	28.26	12.17	19.50

* MM$–millions in US dollars.

Reducing the total capital expenditure by 25% in Case 1 results in a positive NPV0, positive NPV7, and positive IRR of 26.51%. Likewise, increasing the total capital expenditure by 25% in Case 2 still results in positive NPV0, positive NPV7, and IRR of 18.96%. If the product price is reduced by 50% to 0.60 USD/pc in Case 3, the project will not be feasible with a negative net present value at the return rate of 7%. However, if the product price is reduced by only 40% to 0.72 USD/pc in Case 4, the project will yield a positive NPV0, positive NPV7, and positive IRR of 9.79%. Additionally, if the product price can be increased by 50% to 1.80 USD/pc in Case 5, the project will yield significantly high positive NPV0 and NPV15, and a relatively high IRR of 30.36%. The analysis shows the insensitivity of the OPC and HL costs in the economic analysis. If the OPC cost is increased by 20%, as in Case 6, the project's profitability can still be realized by the positive NPV0 and NPV7, and IRR of 22.05%. Furthermore, even with a combination of a 20% increment in OPC and a 20% increment in HL cost in Case 7, the project analysis shows the viability of the success with an IRR of 21.79%. However, reducing the production rate by 50% in Case 8 will result in negative NPV15 and IRR of only 4.39%. Case 9 shows that the production rate can be reduced only by about 15% to 2125 pc/hour, yielding an IRR of 18.51%. The project is more profitable if fixed cost can be reduced by 25%, as in Case 10, which will yield positive NPV0 and NPV7, and IRR of 24.68. Nevertheless, if there are any unprecedented events, such as a shortage in the workforce, the labor rates will go up, leading to an increase in fixed cost by 25%, and the project will still generate positive NPV0 and NPV7, and an IRR of 19.50%.

In summary, the project's robustness is evident when dealing with cost and operational variations, highlighting its adaptability to changing circumstances. However, it underscores the importance of maintaining reasonable product prices and production rates to ensure economic feasibility, as substantial deviations in these areas pose significant challenges to project profitability and overall success.

5.3. Techno-Economic (TE) Analysis of Stone Veneer

The size of the U.S. stone market was 630 million as of 2021 [72], and the scenario in this study is expected to capture approximately 2.3% of the total market size i.e., revenue of USD 14.4 million. For a unit producing 4,800,000 pieces of stone veneer (L 193 × B 89 × T 40 mm) per year, which is equivalent to 3832 metric tons (4224 US tons) of stone veneer from PC, OPC type I, SF, SP, and HL, the total capital expenditure is estimated at USD 10,786,716. The total capital expenditure encompasses the direct cost and indirect cost. Table 7 summarizes the annual production cost estimates for 3832 metric tons (4224 US tons) of stone veneer. The direct cost of USD 4,536,279.16 is estimated based on the equipment and components required for the manufacturing, along with the purchase of land and the construction of a factory. Direct costs, covering equipment, land acquisition, and construction, align closely with the thin brick project with an identical total expenditure of USD 3,861,349.34. The indirect cost of USD 490,436.84 is estimated for the first plant, with many uncertainties in manufacturing the stone veneer (estimated at 90% of the equipment and component purchase cost). The indirect cost includes engineering services, equipment rentals, procurement, freight, taxes, and contingencies. It should be noted that the indirect cost can be reduced when the project maturity increases.

For a product price of 3.0 USD/pc or 129.17 USD/sq. m. (12 USD/sq. ft.) for char-based stone veneer, which is comparable to the price of equivalent commercial stone veneer, as shown in Table 8, the total revenue is estimated at USD 14,400,000/year. Taking 20% of the total revenue, the working capital and startup capital are estimated each at USD 2,880,000. The comparatively high market cost of stone veneer compared to thin bricks is associated with their cost of production. Thin bricks of desired texture and thickness can be produced efficiently using a compression machine alone. On the other hand, the manufacturing of stone veneers requires manual chipping of materials from their sides in addition to the initial casting of rectangular blocks. This labor-intensive process incurs additional costs, making the market price higher. However, the cost of stone veneer manufacturing is lower than the cost of processing natural stone. Natural stone extraction involves quarrying from the mines and then precision cutting, contributing to higher labor costs, whereas the stone veneer production process is more streamlined, and uses molds to make stone veneers of desired size, thereby eliminating the need of quarrying and cutting. It is important to note that the comparison in labor cost is also affected by the geographic locations and tools available for operations.

Table 7. Summary of cost estimates for producing 3832 metric tons (4224 US tons) of stone veneers per year.

Item	Description	Amount
A	Total capital expenditure (i.e., total Cap Ex)	USD 10,786,716.00
	Direct expenditure of total Cap Ex	USD 4,536,279.16
	Indirect expenditure of total Cap Ex	USD 490,436.84
	Working capital at 20% of total revenue (only in year 0)	USD 2,880,000.00
	Startup cost at 20% of total revenue (only in year 1)	USD 2,880,000.00
B	Raw materials (char, cement, silica fume, and SP)	775,648.95 USD/year
	Utility (water and electricity)	15,591.65 USD/year
	Subtotal	791,240.60 USD/year
C	Labor (total 1920 h per year) + Administrative cost	1,120,788.48 USD/year
	Maintenance (4% of Cap Ex)	431,468.64 USD/year
	Lab support cost (5% of Labor)	56,039.42 USD/year
	Plant overhead (10% of labor, maintenance, and lab)	160,829.65 USD/year
	Taxes and insurance (1% of Cap Ex)	107,867.16 USD/year
	Subtotal	1,876,993.36 USD/year
D	Total manufacturing cost (fixed cost + variable cost)	2,668,233.96 USD/year
E	Total manufacturing cost (fixed cost + variable cost)	0.56 USD/pc
F	Product price	3.00 USD/pc
G	Total revenue	14,400,000.00 USD/year

Table 8. Price per square foot of commercial stone veneers.

Manufacturing Company	Price per sq. m.	Price per sq. ft.
Satori 4.41-sq ft Seaside Coast	USD 85.36	USD 7.93 [73]
Clip Stone	USD 158.12	USD 14.69 [74]
Evolve Stone	USD 150.26	USD 13.96 [75]
Average price	USD 129.17	USD 12.19 ≈ USD 12.0

Our research outcomes indicate that 5202.14 tons of total raw materials (including water) are required to yield 4224 tons of stone veneers. For the stone veneer consisting of 1PC:1.34OPC:0.13SF:0.03SP:0.04HL, 1781.54 tons of PC, 2381.54 tons of OPC, 240 tons of SF, 53.54 tons of SP, and 592.80 tons of HL are required per year. Hence, based on the same unit prices of these materials as those used for thin bricks, the yearly cost of purchasing a PC is USD 71,261.54, the yearly cost of purchasing OPC is USD 285,784.62, the yearly cost of purchasing SF is USD 33,600, the yearly cost of purchasing SP is USD 48,184.62, and the yearly cost of purchasing HL is USD 336,818.18. The unit water cost is determined at 1.22 USD/Tliters (4.63 USD/Tgallons) and a fixed monthly cost of USD 127.04 [69]. The total water required in one year (11 working months) to produce 3832 metric tons (4224 US tons) of stone veneers is calculated as 229 Tliters (60.53 Tgallons), including an additional 50% for some other applications, and the total annual water cost is estimated at USD 1677.67. The total electricity consumption to produce 3832 metric tons (4224 US tons) of stone veneer (11 working months) is determined as 143,184 kWh, and the total electricity cost is estimated at 13,913.97 USD/year based on the same rate of electricity as that used for thin bricks. Adding all variable costs yields a total variable cost of 791,240.60 USD/year (Table 7). The fixed cost is determined using a methodology like the one applied in thin bricks, amounting to USD 1,876,993.36, as shown in Table 7. Combining the total fixed and variable costs, the total manufacturing cost is 2,668,233.96 USD/year. This is equivalent to 631.68 USD/ton, which breaks down as 0.56 USD/pc or 32.65 USD/sq. m. (3.03 USD/sq. ft.).

The analysis shows that the percent breakdown of the annual manufacturing cost of USD 2,668,233.96 consists of a total fixed cost of USD 1,876,993.36 (63.3%) and a total variable cost of USD 791,240.60 (36.7%). The variable cost consists of PC cost (2.67%), OPC cost (10.71%), SF cost (1.26%), SP cost (1.81), HL cost (12.62%), water (negligible), and electricity (0.01%). These combined OPC and HL costs, exceeding 20% of the total manufacturing cost, play a significant role in the TE analysis, determining the feasibility of this project. Likewise, the analysis shows that the combined OPC and HL cost is 79% of the total variable cost, further signifying the importance of the combined OPC and HL cost in this project.

The cash flow analysis is conducted similarly to how it is carried out for thin bricks. The cumulative cash flow begins at a negative value of −USD 2,700,000 in Year −2 and reaches the maximum negative value of −USD 13,670,000 in Year 0, before reaching breakeven in Year 2.5, as shown in Figure 18. Similar to thin bricks, the discount rate of 7%, which is higher than the current discount rate of 5.5% [71], is used considering the potential fluctuation in market conditions. With the percent return or discount rate of 7%, the annual cash flow is reduced to the present value, as shown in Figure 19. Likewise, the present yearly value is accumulated, and the cumulative current value is plotted in Figure 19. The cumulative present value begins at −USD 3,090,000 in Year −2, reaches the maximum negative value of −USD 14,430,000 in Year 0, and breakeven in Year 3.

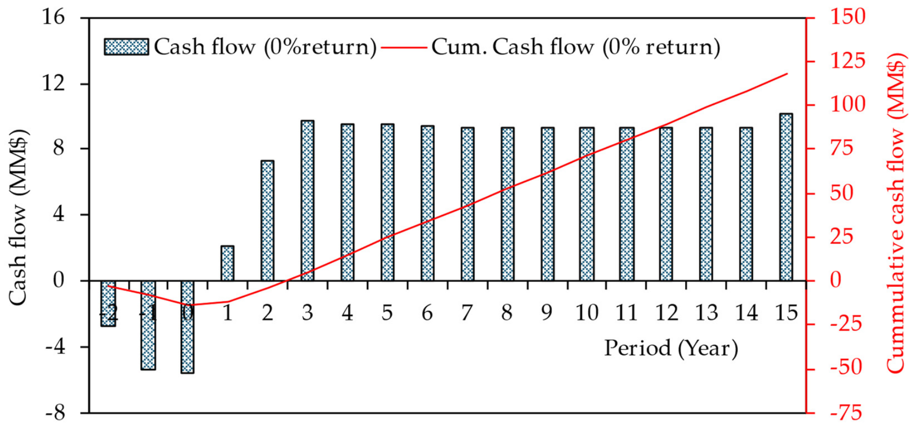

Figure 18. The cash flow analysis results for stone veneer production considering a 0% return.

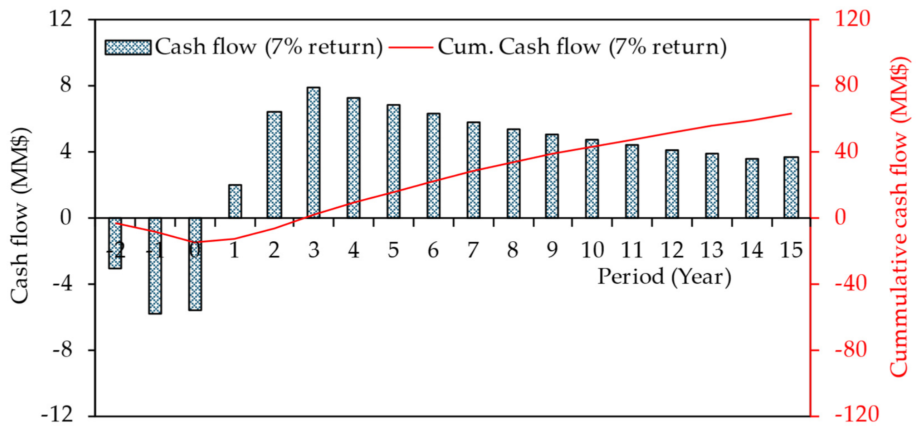

Figure 19. The cash flow analysis results for stone veneers considering a 7% return.

5.4. Sensitivity Analysis for Stone Veneer

Table 9 shows the ten cases and the base case described in previous paragraphs. The sensitivities are evaluated in terms of net present values (i.e., cumulative present value) in Year 15 for 0% and 7% return rates (NPV0 and NPV7), respectively.

Table 9. Sensitivity studies for stone veneers on the net present value and the internal rate of return across varied capital expenditure, production rate, product price, and raw material costs.

Case	Capital Expenditure (MM$ *)	Product Rate (Nos./hour)	Product Price (USD/pc)	Ordinary Portland Cement Cost (USD/ton)	Hydrophobic Liquid Cost (USD/ton)	NPV0 (MM$)	NPV7 (MM$)	IRR (%)
Base	10.76	2500	3.00	120.00	1136.36	118.14	62.68	38.16
1	8.07	2500	3.00	120.00	1136.36	120.27	65.09	44.28
2	13.45	2500	3.00	120.00	1136.36	116.01	60.26	33.71
3	10.76	2500	1.50	120.00	1136.36	43.78	20.97	25.11
4	10.76	2500	4.50	120.00	1136.36	192.5	104.38	44.03
5	10.76	2500	3.00	144.00	1136.36	117.5	62.3	38.02
6	10.76	2500	3.00	144.00	1363.64	116.74	61.85	37.86
7	10.76	2500	3.00	144.00	2727.27	114.35	60.43	37.34
8	10.76	1250	3.00	120.00	1136.36	43.78	20.97	25.11
9	10.76	2500	3.00	144.00	1136.36	123.7	66.05	39.53
10	10.76	2500	3.00	144.00	1363.64	112.58	59.3	36.76

* MM$–millions in US dollars.

Reducing the total capital expenditure by 25% in Case 1 results in a positive NPV0, positive NPV7, and positive IRR of 44.28%; similarly, increasing the total capital expenditure by 25% in Case 2 still results in positive NPV0, positive NPV7, and IRR 33.71%. If the product price is reduced by 50% to 1.50 USD/pc in Case 3, the project will still be feasible with a positive net present value at the return rate of 25.11%. Additionally, if the product price can be increased by 50% to 4.5 USD/pc in Case 4, the project will yield positive NPV0 and NPV7, and a relatively high IRR of 44.03%. The analysis shows the insensitivity of the OPC and HL costs in the economic analysis. If the OPC cost is increased by 20%, as in Case 5, the project's profitability can still be realized by the positive NPV0 and NPV7, and IRR of 38.02%. Likewise, even with a combination of a 20% increment in OPC and a 20% increment in HL cost in Case 6, the project analysis shows the viability of the success with an IRR of 37.86%. Furthermore, even if the cost of HL is increased by two times, as in Case 7, then the profitability of the project can be realized with an IRR of 25.11%. Furthermore, reducing the production rate by 50% in Case 8 will still result in a positive NPV7 and IRR of 25.11. The project stands to be more profitable if fixed cost can be reduced by 25% as in Case 9, which will yield positive NPV0 and NPV7, and IRR of 39.53%. Nevertheless, if there are any unprecedented events, such as a shortage in the workforce, the labor rates will go up, leading to an increase in fixed cost of 25%, and the project will still generate a positive NPV0 and NPV7, and an IRR of 36.76%. In summary, the project's robustness is evident when dealing with cost and operational variations, highlighting its adaptability to changing circumstances.

6. Limitations of the Present Study and Future Works

We acknowledge the limitations in conducting the comparison study with the limited selective set of commercial products. In addition, the economic study is carried out based on the assumption that the factory is running at full capacity, which may not be practical, and we recommend further study to relate to actual site conditions. The costs for disposal of waste products during the operation of the factory are also not considered in this study. This study only aimed to show the possibility of commercialization of char-based thin bricks and stone veneers in manufacturing. Future market studies considering competitors' manufacturing cost and other required factors are suggested to provide detailed comparison. Additionally, study of the micro-/meso-structures of these materials using Computed

Tomography [76], and material characterization using Scanning Electron Microscope and other advanced tools [77], are suggested for future study.

7. Conclusions

The study supports the potential use of char and illustrates its beneficial impact on the engineering properties and economic feasibility. The study finds char-based thin brick and stone veneers to be lightweight, durable, and economical construction products. Compared to commercial products, char-based thin bricks and stone veneers have comparable or better engineering performances in terms of compressive strength, water absorption, freeze–thaw durability, shear bond, and linear shrinkage properties, and these are listed below:

(1) The treated char-based thin bricks and stone veneers showed comparatively low water absorption in the range of 4% to 6%, which is in fair comparison to many commercial products.
(2) The treated char-based thin bricks and stone veneers sustained 50 freeze–thaw cycles in accordance with the ASTM standards C67 [38] and C666 [39], respectively.
(3) As per ASTM C1088, untreated thin brick samples with thicknesses ranging from 13 mm to 22 mm also confirmed their suitability for their application based on their promising freeze–thaw performance.
(4) Stone veneer samples are found to have a low shrinkage ratio of 0.01%, much lower than the ASTM C1670 [4] requirement of 0.1%, further enhancing the durability of this product when used for its intended applications.
(5) When tested for shear bond strength, stone veneer samples have a shear bond strength of 0.75 MPa, 2.73 MPa, and 2.82 MPa depending upon the type of adhesive used, which is well above the ASTM C1670 [4] requirement of 0.35 MPa. Moreover, compared to commercial ones, they have better shear bond strength.
(6) The techno-economic analysis conducted for thin bricks shows the viability of project implementation with a net positive NPV0 and NPV7, along with an IRR of 22.15%. These economic indicators justify the adaptability of the project implementation even with the changing market conditions, as validated by a sensitivity study.
(7) However, the project's success for thin brick is contingent on the product price and production rate. The analysis shows that the product price of USD 0.60 will lead the project to some loss, giving a return of only 4.39%. In addition, when the production rate is reduced by half, the return rate is reduced to 4.39%.
(8) For stone veneers, all the economic parameters are positive, and IRR is 38.16%, which justifies their ability to sustain the fluctuating market conditions.
(9) The sensitivity analysis performed for stone veneer also showed positive NPV0 and NPV7, and IRR of 25.11% even when the product prices are reduced to half, or the production rate is reduced to half.

This study demonstrates that char-based thin brick and stone veneer are viable alternatives to conventional building materials due to their favorable engineering properties and promising economic viability.

8. Patents

The content presented in this manuscript is part of the provisional patent application No. 63/439,527.

Author Contributions: Conceptualization, H.Y. and K.N.; methodology, validation, S.P.P.; formal analysis, S.P.P.; investigation, S.P.P. and C.L.; resources, C.L.; writing—original draft preparation, S.P.P.; writing—review and editing, H.Y., C.L. and K.N.; supervision, K.N.; project administration, C.L.; funding acquisition, K.N. All authors have read and agreed to the published version of the manuscript.

Funding: This research was funded by the Wyoming State Legislator through the School of Energy Resources of the University of Wyoming.

Institutional Review Board Statement: Not applicable.

Informed Consent Statement: Not applicable.

Data Availability Statement: Data are contained within the article.

Conflicts of Interest: The authors declare no conflict of interest.

References

1. Park, J.; Kim, S.; Mun, J.; Yang, K.; Sim, J. Shaking Table Tests of Veneer Masonry Wall Retrofitted with Long-raw Plug Screw Anchors. *J. Build. Eng.* **2023**, *76*, 107163. [CrossRef]
2. Marziale, S.A.; Toubia, E.A. Analysis of Brick Veneer on Concrete Masonry Wall Subjected to In-Plane Loads. *Structures* **2015**, *2*, 1–7. [CrossRef]
3. *ASTM C1088-23*; ASTM 2023 Standard Specification for Thin Veneer Brick Units Made from Clay or Shale. ASTM: West Conshohocken, PA, USA, 2023.
4. *ASTM C1670/C1670M-23*; ASTM 2023 Standard Specification for Adhered Manufactured Stone Masonry Veneer Units. ASTM: West Conshohocken, PA, USA, 2023.
5. Vanpachtenbeke, M.; Langmans, J.; Bulcke, J.V.D.; Acker, J.V.; Roles, S. On the Drying Potential of Cavity Ventilation Behind Brick Veneer Cladding: A Detailed Field Study. *Build. Environ.* **2017**, *123*, 133–145. [CrossRef]
6. Martins, A.; Vasconcelos, G.; Costa, A.C. Brick Masonry Veneer Walls: An Overview. *J. Build. Eng.* **2017**, *9*, 29–41. [CrossRef]
7. M S International Inc. Real Stone Vs. Stone Veneer: What's the Difference? 2019. Available online: https://www.msisurfaces.com/blogs/post/2019/06/28/real-stone-vs-stone-veneer-whats-the-difference.aspx (accessed on 17 October 2023).
8. Forest Service U.S. Department of Agriculture. Available online: https://www.fs.usda.gov/research/treesearch/34288 (accessed on 3 February 2024).
9. Paragon Tools. Brick Veneer Lifespan and Maintenance: What You Need to Know. Available online: https://www.paragontools.ie/how-long-does-brick-veneer-last/ (accessed on 5 October 2023).
10. Wei, S.; Jiang, Z.; Liu, H.; Zhou, D.; Silva, M. Microbiologically Induced Deterioration of Concrete—A Review. *Braz. J. Microbiol.* **2013**, *44*, 1001–1007. [CrossRef]
11. Noeiaghaei, T.; Mukherjee, A.; Dhami, N.; Chae, S. Biogenic Deterioration of Concrete and Its Mitigation Technologies. *Constr. Build. Mater.* **2017**, *149*, 575–586. [CrossRef]
12. Safiuddin, M. Concrete Damage in Field Conditions and Protective Sealer and Coating Systems. *Coatings* **2017**, *7*, 90. [CrossRef]
13. Wang, H.; Long, G.; Xie, Y.; Zeng, X.; Ma, K.; Dong, R.; Tang, Z.; Xiao, Q. Effects of Intense Ultraviolet Irradiation on Drying Shrinkage and Microstructural Characteristics of Cement Mortar. *Constr. Build. Mater.* **2022**, *347*, 128513. [CrossRef]
14. Diversified Builder Supply Inc. Different Types of Stone Veneers 2022. Available online: https://www.dbsincaz.com/different-types-stone-veneers/ (accessed on 20 October 2023).
15. Brick My Walls.com. Clay Brick Veneer. Available online: https://www.brickmywalls.com/product-category/brick-veneer-clay-based/ (accessed on 21 October 2023).
16. Ozcelik, M. Energy Consumption Analysis for Natural Aggregate Processing and its Results (Atabey, Isparta, Turkey). *Min. Miner. Depos.* **2018**, *12*, 80–86. [CrossRef]
17. Zegardlo, B. Comparative Assessment of Environmental Effects by LCA Method of Natural Aggregates Extraction Processes and Production of their Substitutes from Waste in the City Mining System. *J. Ecol. Eng.* **2021**, *22*, 251–257. [CrossRef] [PubMed]
18. Ngom, M.; Thiam, A.; Balhamri, A.; Sambou, V.; Raffak, T.; Refaey, H.A. Transient Study During Clay Bricks Cooking in the Traditional Kiln; CFD Numerical Study. *Case Stud. Therm. Eng.* **2021**, *28*, 101672. [CrossRef]
19. Khan, M.W.; Ali, Y.; Felice, F.D.; Salman, A.; Petrillo, A. Impact of Brick Kilns Industry on The Environment and Human Health in Pakistan. *Sci. Total Environ.* **2019**, *678*, 383–389. [CrossRef]
20. Mohammad, S.A.; Koting, S.; Katman, H.Y.B.; Babalghaith, A.M.; Patah, M.F.A.; Ibrahim, M.R.; Karim, M.R. A Review of the Utilization of Coal Bottom Ash (CBA) in the Construction Industry. *Sustainability* **2021**, *13*, 8031. [CrossRef]
21. Seav, N.; Kim, K.S.; Kim, K.S.; Lee, S.W.; Kim, Y.K. Effects of Roller Compacted Concrete Incorporating Coal Bottom Ash as a Fine Aggregate Replacement. *Sustainability* **2023**, *15*, 11420. [CrossRef]
22. Zhang, D.; Zhang, S.; Yang, Q. Effect of Replacing Fine Aggregate with Fly Ash on the Performance of Mortar. *Materials* **2023**, *16*, 4292. [CrossRef]
23. U.S. Energy Information Administration. U.S. Coal-Fired Generation Declining after Brief Rise in Last Year. Available online: https://www.eia.gov/todayinenergy/detail.php?id=54419 (accessed on 3 February 2024).
24. Zhang, Y.; Zou, X.; Zhao, H. A Clean Coal Utilization Technology Based on Coal Pyrolysis and Chemical Looping with Oxygen Uncoupling: Principle and Experimental Validation. *Energy* **2016**, *98*, 181–189. [CrossRef]
25. Wu, F.; Huang, S.; Jiang, Q.; Jiang, G. Effects of Pressure and Heating Rate on Coal Pyrolysis: A Study in Simulated Underground Coal Gasification. *J. Anal. Appl. Pyrolysis* **2023**, *175*, 106179. [CrossRef]
26. Ramalingam, S.; Subramanian, S.; Subramanian, A. Utilization of Pyrolytic Oil and Hydrogen Enriched Syngas from Single Feedstock (Delonix Regia) through Pyrolysis Process and its Influence on Performance and Emission Characteristics in CI Engine. *Int. J. Hydrog. Energy* **2022**, *47*, 36749–36762. [CrossRef]
27. Yu, H.; Joshi, P.; Lau, C.; Ng, K. Novel Application of Sustainable Coal-Derived Char in Cement Soil Stabilization. *Constr. Build. Mater.* **2024**, *414*, 134960. [CrossRef]

28. Ramasubramani, R.; Gunasekaran, K. Sustainable Alternate Materials for Concrete Production from Renewable Source and Waste. *Sustainability* **2021**, *13*, 1204. [CrossRef]
29. Olayiwola, S.O.; Ng, K. Influence of Fly-Ash Reaction on the Performance of Coal-Derived Char Bricks. *J. Mater. Civ. Eng.* **2023**, *35*, 04023337–1-13. [CrossRef]
30. Yu, H.; Jonchhe, P.; Lau, C.; Ng, K. Temperature Effect on Density, Strength, and Microstructure of Sustainable Coal Char-Cement Grout. *J. Build. Eng.* **2023**, *80*, 107975. [CrossRef]
31. Yu, H.; Ng, K.; Lau, C. New Coal Char-Based Bricks: Effects of Curing Temperature, Humidity, Pressing Pressure, and Addition of Superplasticizer on the Physical, Mechanical, and Thermal Properties. *Case Stud. Constr. Mater.* **2023**, *19*, e02529. [CrossRef]
32. Yu, H.; Kharel, S.; Lau, C.; Ng, K. Development of High-Strength, and Durable Coal Char-Based Building Bricks. *J. Build. Eng.* **2023**, *74*, 106908. [CrossRef]
33. Kanchanapiya, P.; Methacanon, P.; Tantisattayakul, T. Techno-Economic Analysis of Light Weight Concrete Block Development from Polyisocyanurate Foam Waste. *Resour. Conserv. Recycl.* **2018**, *138*, 313–325. [CrossRef]
34. Khan, M.I.; Abbas, Y.M.; Fares, G. Enhancing Cementitious Concrete Durability and Mechanical Properties through Silica Fume and Micro-Quartz. *Sustainability* **2023**, *15*, 15913. [CrossRef]
35. Arch Daily. Thin Brick in Building Design: A Guide to Their Use and Application. Available online: https://www.archdaily.com/1008409/thin-brick-in-building-design-a-guide-to-their-use-and-application (accessed on 27 October 2023).
36. *ASTM C31/C31M-23*; ASTM 2023 Standard Practice for Making and Curing Concrete Test Specimens in the Field. ASTM: West Conshohocken, PA, USA, 2023.
37. *ASTM C39/C39M-21*; ASTM 2021 Standard Test Method for Compressive Strength of Cylindrical Concrete Specimens. ASTM: West Conshohocken, PA, USA,, 2021.
38. *ASTM C67/C67M-23a*; ASTM 2023 Standard Test Methods for Sampling and Testing Brick and Structural Clay Tile. ASTM: West Conshohocken, PA, USA, 2023.
39. *ASTM C666/C666M-15*; ASTM 2016 Standard Test Method for Resistance of Concrete to Rapid Freezing and Thawing. ASTM: West Conshohocken, PA, USA, 2016.
40. *ASTM C157/C157M-17*; ASTM 2017 Standard Test Method for Length Change of Hardened Hydraulic-Cement Mortar and Concrete. ASTM: West Conshohocken, PA, USA, 2017.
41. *ASTM C482-20*; ASTM 2020 Standard Test Method for Bond Strength of Ceramic Tile to Portland Cement Paste. ASTM: West Conshohocken, PA, USA, 2020.
42. Arunachelam, N.; Maheswaran, J.; Chellapandian, M.; Murali, G.; Vatin, N.I. Development of High-Strength Geopolymer Concrete Incorporating High-Volume Copper Slag and Micro Silica. *Sustainability* **2022**, *14*, 7601. [CrossRef]
43. Rizaee, S.; Shrive, N. Shear Bond Strength of Adhered Thin Masonry Veneer with Traditional and Polymer Modified Mortars. *Constr. Build. Mater.* **2023**, *379*, 131277. [CrossRef]
44. Kulaots, I.; Aarna, I.; Callejo, M.; Hurt, R.H.; Suuberg, E.M. Development of Porosity During Coal Char Combustion. *Proc. Combust. Inst.* **2002**, *29*, 495–501. [CrossRef]
45. Yang, H.; Pisupati, S.V.; Hu, H. Modeling Char Surface Area Evolution During Coal Pyrolysis: Effect of Swelling and Gasification at High Pressures. *Proc. Combust. Inst.* **2021**, *38*, 4151–4159. [CrossRef]
46. Ivanova, I.; Mechtcherine, V. Effects of Volume Fraction and Surface Area of Aggregates on the Static Yield Stress and Structural Build-Up of Fresh Concrete. *Materials* **2020**, *13*, 1551. [CrossRef]
47. Hover, K.C. The Influence of Water on the Performance of Concrete. *Constr. Build. Mater.* **2011**, *25*, 3003–3013. [CrossRef]
48. Hita, M.J.D.; Criado, M. Influence of superplasticizers on the workability and mechanical development of binary and ternary blended cement and alkali-activated cement. *Constr. Build. Mater.* **2023**, *366*, 130272. [CrossRef]
49. Zhang, H.; Huang, Y.; Xu, S.; Hu, X.; Zheng, Z. 3D Cohesive Fracture of Heterogeneous CA-UHPC: A Mesoscale Investigation. *Int. J. Mech. Sci.* **2023**, *249*, 108270. [CrossRef]
50. Quality Stone Veneer, Inc. *Product Technical Specs*. 2023. Available online: https://canyonstonecanada.com/Home/TechDocs (accessed on 15 November 2023).
51. Canyon Stone Canada. Technical Specifications. 2023. Available online: https://www.qualitystoneveneer.com/technical-specs (accessed on 15 November 2023).
52. The Belden Brick Company. Belcrest 760. Available online: https://www.beldenbrick.com/brick/thin-brick-colors/color/texture/mm/size/series/finish/belcrest_760 (accessed on 10 September 2023).
53. Anh, L.D.H.; Pasztory, Z. An Overview of Factors Influencing Thermal Conductivity of Building Insulation Materials. *J. Build. Eng.* **2021**, *44*, 102604.
54. Keskin, M.S.; Bildik, S.; Laman, M. Experimental and Numerical Studies of Vertical Stresses Beneath the Circular Footings on Sand. *Appl. Sci.* **2023**, *13*, 1635. [CrossRef]
55. LI, W.; Pour-Ghaz, M.; Castro, J.; Weiss, J. Water Absorption and Critical Degree of Saturation Relating to Freeze-Thaw Damage in Concrete Pavement Joints. *J. Mater. Civ. Eng.* **2012**, *24*, 299–307. [CrossRef]
56. Newnan, D.G.; Eschenbach, T.G.; Lavelle, J.P. *Engineering Economic Analysis*; Oxford University Press: New York, NY, USA, 2012.
57. Duke Accounting. Gap 200.090, Plant & Equipment Depreciation. Available online: https://finance.duke.edu/accounting/gap/m200-090 (accessed on 4 February 2024).

58. Ahmed, A.A.; Assadi, M.; Kalantar, A.; Sliwa, A.S.; Sliwa, T.; Ahmed, N.; Rogozik, S. Evaluating the Techno-Economic Impact of Decarbonizing Buildings by Using Borehole Heat Exchangers in Comparison to Fuel-Based Systems. *Energy Sustain. Dev.* **2023**, *76*, 101262. [CrossRef]
59. Precedence Research. Brick Market. Available online: https://www.precedenceresearch.com/bricks-market#:~:text=The%20U.S.%20bricks%20market%20size,3.30%25%20from%202023%20to%202032 (accessed on 2 February 2024).
60. Residential Lot—Gillette, WY. Available online: https://www.landwatch.com/campbell-county-wyoming-undeveloped-land-for-sale/pid/416036264 (accessed on 20 December 2023).
61. Construction Cost Estimates for Factory, 1 Story in National, US. Available online: https://www.rsmeans.com/model-pages/factory-1-story (accessed on 20 December 2023).
62. Tiles Direct. Brickwork. Available online: https://www.tilesdirect.net/categories/daltile/brickwork (accessed on 5 December 2023).
63. Menards, Inc. VersaTILE®Royal Thin Brick®Hawthorn 2-3/4 × 7-5/8 Tumbled Thin Brick Veneer Floor and Wall Tile. Available online: https://www.menards.com/main/flooring-rugs/tile-stone/quarry-tile/versatile-reg-royal-thin-brick-reg-2-3-4-x-7-5-8-tumbled-thin-brick-veneer-floor-and-wall-tile/458-2348r0-058-wc-mt1/p-1523341810465-c-6560.htm (accessed on 8 December 2023).
64. Lau, C.K. Investigating the Lifecycle Performance and Techno-Economic Analysis of Coal-Derived Carbon Building Materials for Low-Rise Buildings. Master's Thesis, University of Wyoming, Laramie, WY, USA, May 2022.
65. Third Derivative. Bringing Low-Carbon Cement to Market. Available online: https://www.third-derivative.org/blog/low-carbon-cement (accessed on 24 December 2023).
66. Alibaba. Buy 90% Sio2 Densified Concrete Additive Dark Grey Micro Silica for Company of Micro Silica. Available online: https://www.alibaba.com/product-detail/Buy-90-SiO2-Densified-Concrete-Additive_1600734833118.html?s=p (accessed on 27 December 2023).
67. Alibaba. PCE Powder Superplasticizer/PCE Superplasticizer Polycarboxylate Ether. Available online: https://www.alibaba.com/product-detail/PCE-Powder-Superplasticizer-PCE-Superplasticizer-Polycarboxylate_1600969454183.html (accessed on 27 December 2023).
68. Made in China. Hydrophobic Liquid Silway 744 Nano Waterproof Spray for Cement Roof Tiles with High Quality. Hydrophobic Liquid Silway 744 Nano Waterproof Spray for Cement Roof Tiles with High Quality—China Polydimethylsiloxane and Dimethylioxane. Available online: https://hzsilway.en.made-in-china.com/product/aQOUGDkrTfht/China-Hydrophobic-Liquid-Silway-744-Nano-Waterproof-Spray-for-Cement-Roof-Tiles-with-High-Quality.html (accessed on 27 December 2023).
69. Gillette Wyoming. City of Gillette Bill Pay. Available online: https://www.gillettewy.gov/city-government/departments/utilities/utilities-administration/city-of-gillette-bill-pay (accessed on 27 December 2023).
70. U.S. Bureau of Labor Statics. Occupational Employment and Wage Statistics. Available online: https://www.bls.gov/oes/current/oes_wy.htm (accessed on 28 December 2023).
71. Y Charts. US Discount Rates. Available online: https://ycharts.com/indicators/us_discount_rate_monthly (accessed on 5 January 2024).
72. Fortune Business Insights. Building & Construction Materials. Available online: https://www.fortunebusinessinsights.com/u-s-stone-veneer-market-107397 (accessed on 2 February 2024).
73. Lowes. Satori 4.41-sq ft Seaside Coast Stone Veneer. Available online: https://www.lowes.com/pd/Satori-4-41-sq-ft-Seaside-Coast-Stone-Veneer-Stacked-Stone/5002174513 (accessed on 8 December 2023).
74. Menards, Inc. ClipStone®Willow Peak ProStack Manufactured Stone Veneer Siding Flats (5 sq ft). Available online: https://www.menards.com/main/building-materials/siding/stone-veneer-panels-siding/clipstone-reg-prostack-manufactured-stone-veneer-siding-flats-5-sq-ft/css-10-014-40/p-1642874267252502-c-19691.htm (accessed on 14 December 2023).
75. In and Out Home Products. Evolve Stone National True Stone Veneer (14.25 sq. ft. per Box). Available online: https://inandouthome.com/products/xhwent (accessed on 20 December 2023).
76. Huang, Y.; Natarajan, S.; Zhang, H.; Guo, F.; Xu, S.; Zeng, C.; Zheng, Z. A CT Image Driven Computational Framework for Investigating Complex 3D Fracture in Mesoscale Concrete. *Cem. Concr. Compos.* **2023**, *143*, 105270. [CrossRef]
77. Panwar, A.S.; Singh, A.; Sehgal, S. Material Characterization Techniques in Engineering Applications: A Review. *Mater. Today: Proc.* **2020**, *20*, 1932–1937. [CrossRef]

Disclaimer/Publisher's Note: The statements, opinions and data contained in all publications are solely those of the individual author(s) and contributor(s) and not of MDPI and/or the editor(s). MDPI and/or the editor(s) disclaim responsibility for any injury to people or property resulting from any ideas, methods, instructions or products referred to in the content.